Neutrino and anti-neutrino cross sections on ^{18}O and ^{40}Ar within QRPA nuclear models

Arturo R. Samana
UESC-BA- Brazil

in collaboration with
F. Krmpotic, A. Mariano, C. Barbero – UNLP -Argentina
C. A. Bertulani -Texas A&M University – Commerce-USA
N. Paar – University of Zagreb – Croatia
M. Mohammadzadeh, H. Khalili-Faculty of Sciences Arak University - Iran
S. Duarte, M. Santos- CBPF – RJ- Brazil
V. dos S. Ferreira – UFRB - BA - Brazil

08/10/2023

INSTITUTE for NUCLEAR THEORY

Outline

▪ Motivation

- On neutrino physics and nuclear structure.

- Detection of supernovae neutrinos

▪ Weak-Nuclear interaction formalism

▪ Nuclear Models

QRPA and PQRPA

▪ Some numerical results

$\nu_e / \overline{\nu}_e$ 18O and 40Ar cross section

▪ Summary

Motivation

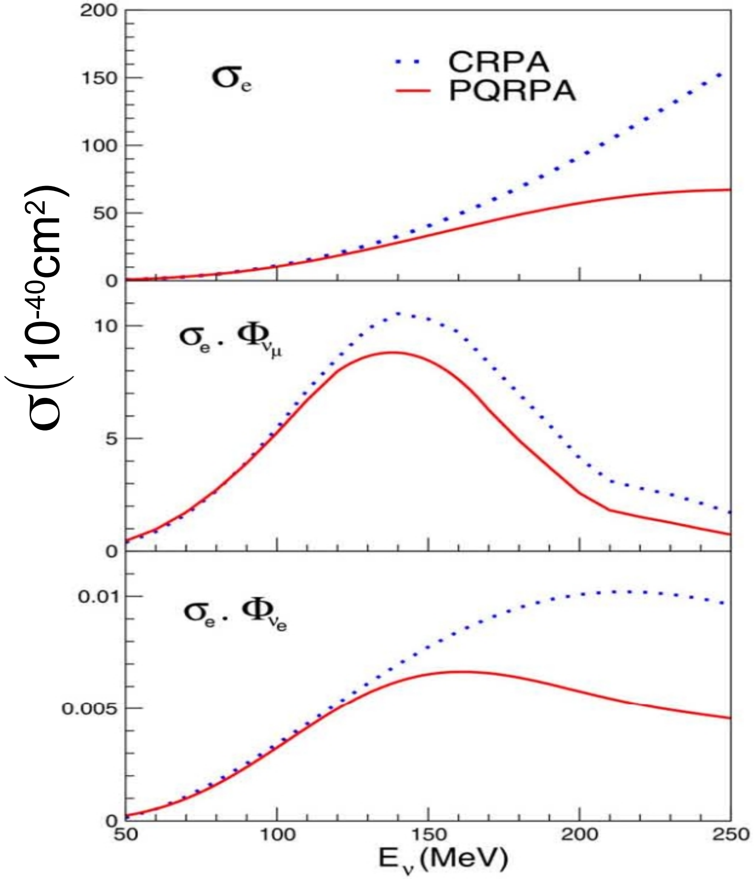

ν-nucleus cross section are important to constrain parameters in neutrino oscillations.

$\bar{\nu}_\mu \rightarrow \bar{\nu}_e \quad \nu_\mu \rightarrow \nu_e$

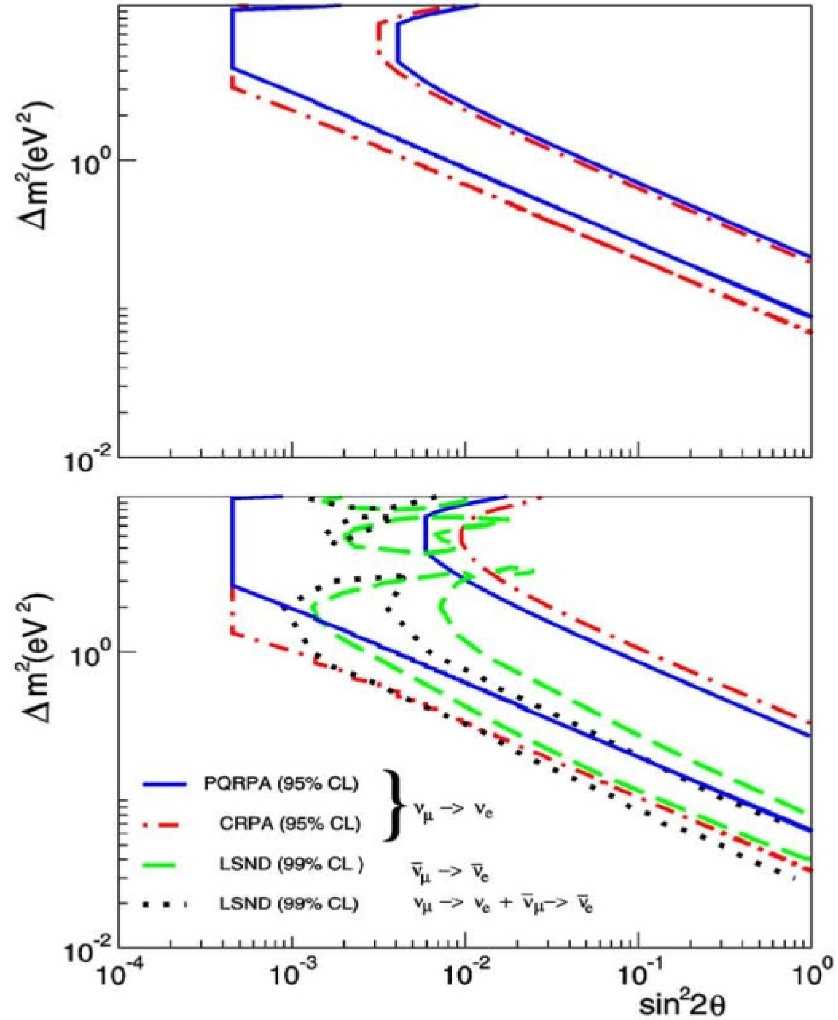

* Increase probability oscillations.
* Confidence level region is diminished by difference in σ_e between PQRPA and CRPA, PLB (2005) 100

Supernovae Neutrinos – Signal Detection

Number of target nuclei — Neutrino flux — Interaction cross section — Efficiency

$$N_{ev} = N_t \int_0^{\infty} F(E_\nu)\cdot\sigma(E_\nu)\cdot\varepsilon(E_\nu)\,dE_\nu$$

SNO

$$\nu_e + d \rightarrow p + p + e^-$$

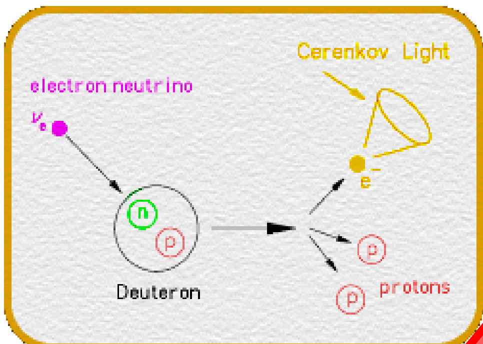

Super-K

$$\nu_e + {}^{16}O \rightarrow {}^{16}F + e^-$$

$$\bar{\nu}_e + {}^{16}O \rightarrow {}^{16}N + e^+$$

$$\bar{\nu}_e + p \rightarrow n + e^+$$

LVD

$$\nu_e + {}^{12}C \rightarrow {}^{12}N + e^-$$

$$\bar{\nu}_e + {}^{12}C \rightarrow {}^{12}B + e^+$$

$$\nu_e + {}^{56}Fe \rightarrow {}^{56}Co + e^-$$

$$\bar{\nu}_e + {}^{56}Fe \rightarrow {}^{56}Mn + e^+$$

$$\sigma(E_\nu) \Leftrightarrow F(E_\nu)$$

Supernovae Neutrinos – Signal Detection

LAr**TPC** - **L**iquid **Ar**gon **T**ime **P**rojection **C**hambers: ν_e-^{40}Ar

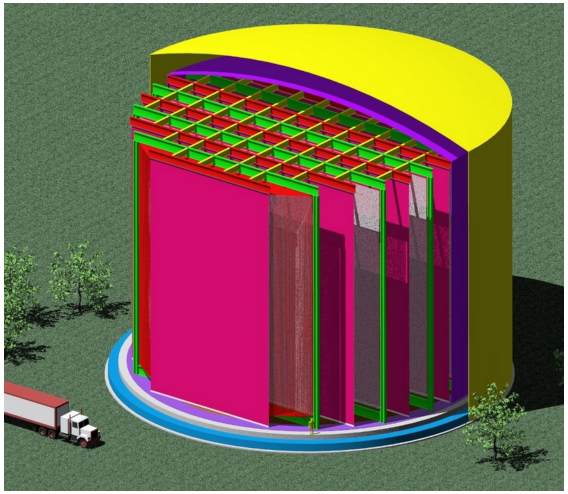

http://www-lartpc.fnal.gov/

RPA: Ormand,Pizzochero, Bortignon, Broglia, PLB 345(343)1995
RPA: Martinez-Pinedo, Kolbe & Langanke K, priv. comm. Gil-Botella & Rubbia, JCAP10 (2003) 009
SM : T. Suzuki & M. Honma, arXiv:1211.4078v1 [nucl-th] 17 Nov 2012
QRPA : M. Cheoun etal , PRC **83,** 028801 (2011)

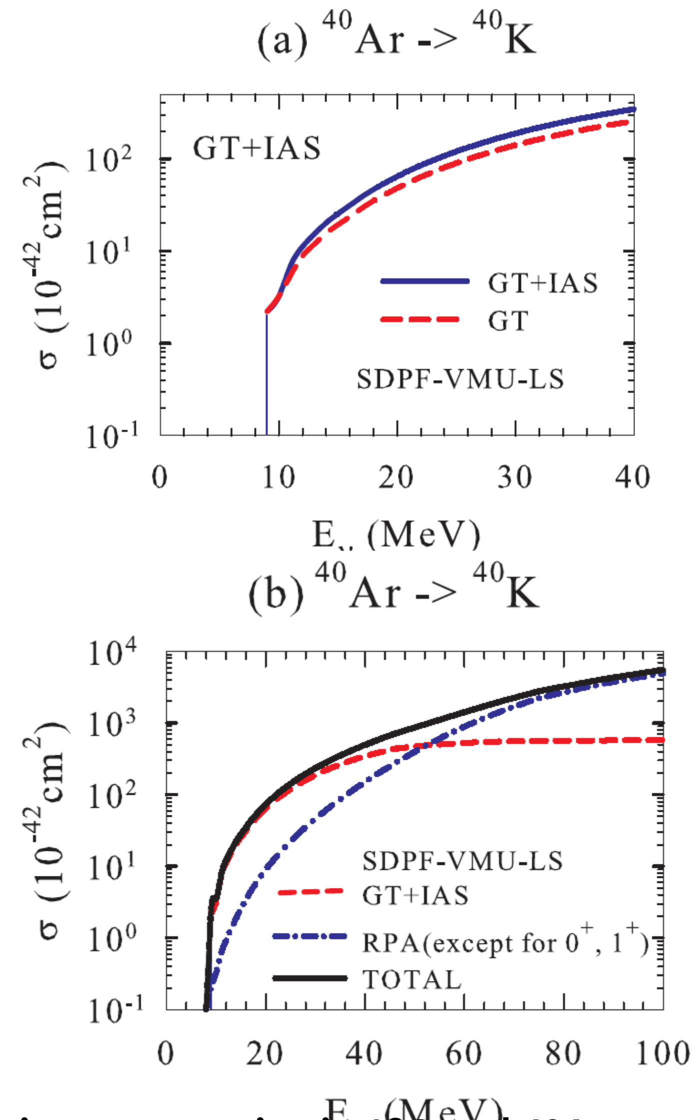

Supernovae Neutrinos – Signal Detection

DUNE - Deep Underground Neutrino Experiment: ν_e - ^{40}Ar

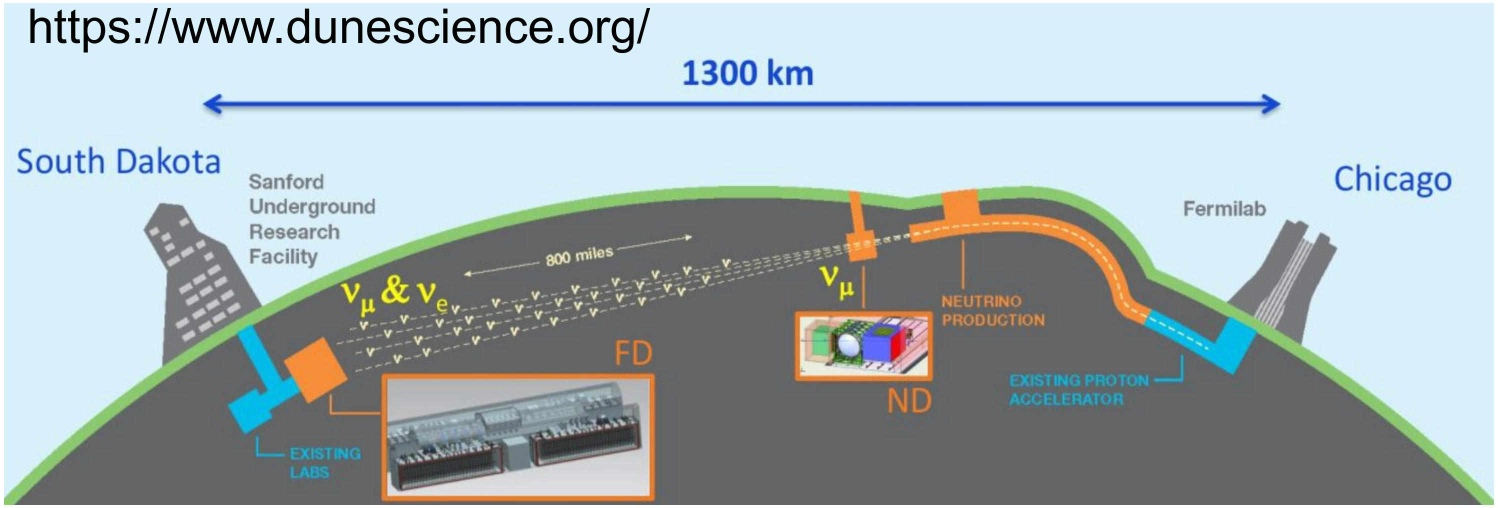

One of the primary physics goals for DUNE is to obtain a high-statistics measurement of core-collapse supernova.

B. Abi et al. (DUNE Collaboration), Eur. Phys. J. C 81, 423 (2021), 982

About ^{18}O on SN and Double Beta Decay

- **^{18}O is a stable isotope of ^{16}O with 0.21 percent of abundance. Present in CNO cycle**

$$^{12}\mathrm{C} + \alpha \rightarrow ^{16}\mathrm{O} + \gamma,$$
$$^{16}\mathrm{O} + \alpha \rightarrow ^{20}\mathrm{Ne} + \gamma,$$
$$^{14}\mathrm{N} + \alpha \rightarrow ^{18}\mathrm{F} + e^{+} + \gamma.$$

$$^{18}\mathrm{F} \rightarrow ^{18}\mathrm{O} + e^{+} + \nu_e,$$

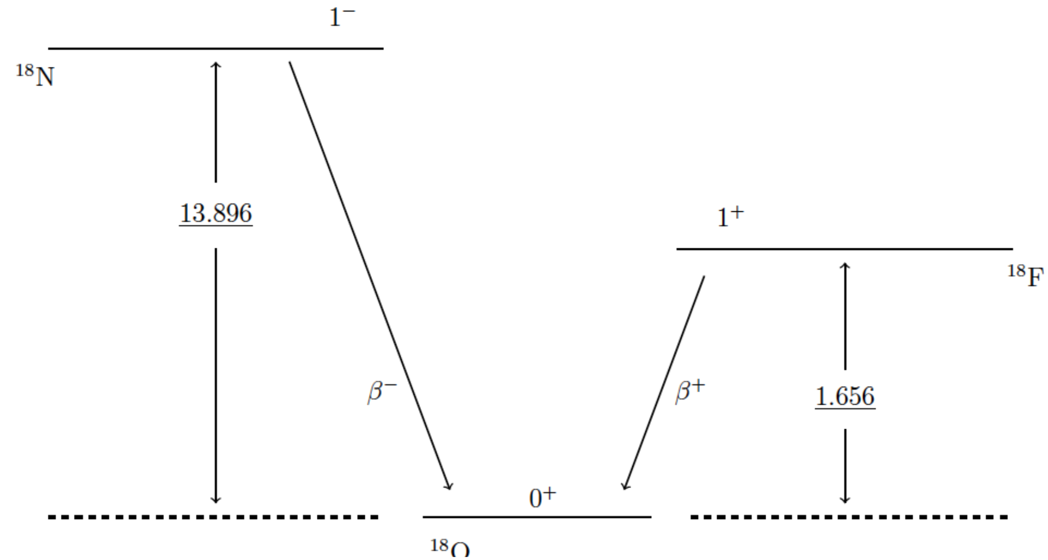

- A good acknowledgement of the nuclear structure of 18O is important for the study of heavy-ion double charge exchange reactions, proposed as a tool to impose limit on 0vββ nuclear matrix elements.
Cappuzzello et al., Eur. Phys. J. A 51, 145 (2015) NUMEN Collaboration

$$^{40}\mathrm{Ca}(^{18}\mathrm{O},^{18}\mathrm{Ne})^{40}$$
$$^{40}\mathrm{Ca}(^{18}\mathrm{O},^{18}\mathrm{F})^{40}$$
$$^{40}\mathrm{Ca}(^{18}\mathrm{O},^{20}\mathrm{Ne})^{38}\mathrm{Ar}$$
$$^{40}\mathrm{Ca}(^{18}\mathrm{O},^{16}\mathrm{O})^{42}\mathrm{Ca}$$

NUMEN

$$^{18}\mathrm{O}(\nu_e, e^-)^{18}\mathrm{F} \text{ and } ^{18}\mathrm{O}(\bar{\nu}_e, e^+)^{18}\mathrm{N}$$

- **No estimations of these cross sections.**

Weak–nuclear interaction

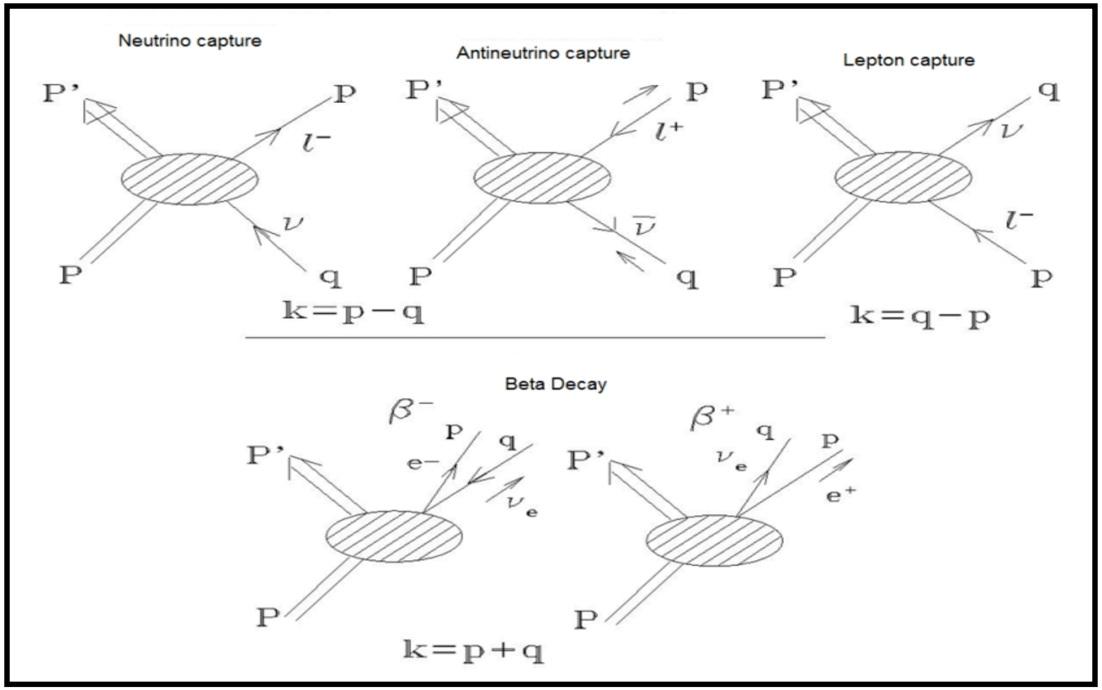

Charged Current

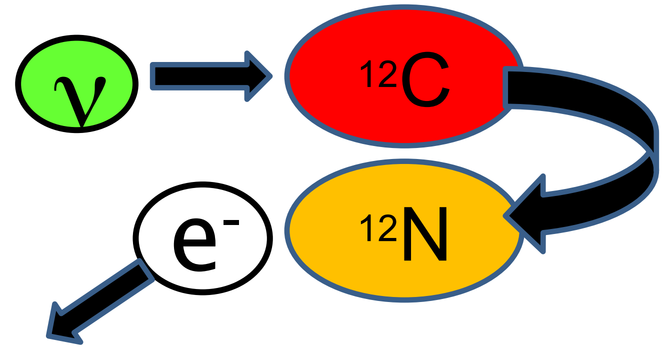

Neutral Current

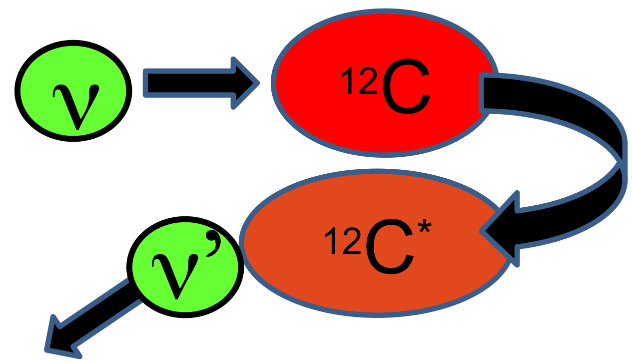

$$\nu_e + A(Z,N) \Rightarrow A^*(Z+1,N-1) + e^-$$

$$\bar{\nu}_e + A(Z,N) \Rightarrow A^*(Z-1,N+1) + e^+$$

(i)O'Connell, Donelly & Walecka, PR6,719 (1972)
(ii) Kuramoto et al. NPA 512, 711 (1990)
(iii) Luyten et al. NP41,236 (1963)
(iv) Krmpotic et al. PRC71, 044319(2005).

ALL ARE EQUIVALENTS.

Weak–nuclear interaction

Reaction:

$$\nu_l + (Z, A) \rightarrow (Z+1, A) + l^-$$

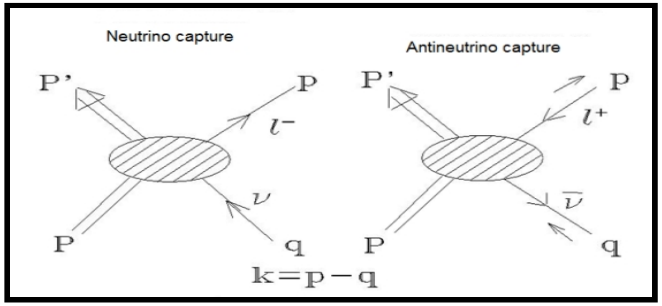

Weak hamiltonian:

$$H_w(\mathbf{r}) = \frac{G}{\sqrt{2}} J_\alpha l^\alpha e^{-ik\cdot r}$$

$$J_\alpha = i\gamma_4 \left[g_V \gamma_\alpha - \frac{g_M}{2\mathrm{M}} \sigma_{\alpha\beta} k_\beta + g_A \gamma_\alpha \gamma_5 + i \frac{g_P}{\mathrm{m}_\ell} k_\alpha \gamma_5 \right]$$

$$l_\alpha = -i \overline{u}_{s_\ell}(\mathbf{p}, E_\ell) \gamma_\alpha (1+\gamma_5) u_{s_\nu}(\mathbf{q}, E_\nu)$$

Neutrino-nucleus cross section (Fermi's Golden Rule):

$$\sigma(E_\nu, J_n^\pi) = \frac{E_e |\mathbf{p_e}|}{2\pi} F(Z+S, E_e) \int_{-1}^{+1} d(cos\theta) \tau(\kappa, J_n^\pi),$$

p_l :Lepton momentum, E_l: Lepton energy, *F(Z+S,E):* Fermi function, S=1 or -1

$$\tau_\sigma(\kappa, \mathrm{J}) = \frac{G^2}{2J_i+1} \left[\sum_J \mathcal{L}_\emptyset |\langle \mathrm{J} || O_\emptyset(J) || J_i \rangle|^2 + \sum_{M=0\pm1} \mathcal{L}_M |\langle \mathrm{J} || O_M(J) || J_i \rangle|^2 \right.$$

Transition amplitude

$$\left. -2Re \left[\langle \mathrm{J} || O_\emptyset(J) || J_i \rangle^* \langle \mathrm{J} || O_0(J) || J_i \rangle \right] \mathcal{L}_{\emptyset 0} \right].$$

$\mathrm{O}_\alpha = \left\langle J_f \,||\, J_\alpha e^{-i\vec{k}\cdot\vec{r}} \,||\, J_i \right\rangle$, Nuclear Matrix Element , $\mathcal{L}_\emptyset$, $\mathcal{L}_M$ and $\mathcal{L}_{\emptyset 0}$ Lepton traces

$k = (\vec{k}, k_\emptyset), \rho = \kappa . r = |\vec{k}| . r$ Transfer momentum, with **k**= |**k**| ž.

Weak–nuclear interaction

Non-relativistic approximation of hadronic current

$$J_\emptyset = g_V + (\overline{g}_A + \overline{g}_{P1})\boldsymbol{\sigma}\cdot\hat{\mathbf{k}} + i g_A \mathrm{M}^{-1}\boldsymbol{\sigma}\cdot\boldsymbol{\nabla},$$

$$\mathbf{J} = -g_A\boldsymbol{\sigma} - i\overline{g}_W\boldsymbol{\sigma}\times\hat{\mathbf{k}} - \overline{g}_V\hat{\mathbf{k}} + \overline{g}_{P2}(\boldsymbol{\sigma}\cdot\hat{\mathbf{k}})\hat{\mathbf{k}} - i g_V \mathrm{M}^{-1}\boldsymbol{\nabla},$$

Nuclear coupling constant

$$g_V = 1, \quad g_A = 1.26,$$ → $g_A \sim 1$

$$g_M = \kappa_p - \kappa_n = 3.70, \quad g_P = g_A\frac{2\mathrm{M}m_\ell}{k^2 + m_\pi^2}.$$

FNS effect: $g \Rightarrow g\left(\frac{\Lambda^2}{\Lambda^2 + k^2}\right)^2$

Λ=850 MeV

Transfer momentum, with **k**= |**k**| ž.

$$e^{-i\mathbf{k}\cdot\mathbf{r}} = \sum_L i^{-L}\sqrt{4\pi(2L+1)}\, j_L(\kappa r) Y_{L0}(\hat{\mathbf{r}}),$$

Elementary Operators :

$$\mathcal{M}^V_J = j_J(\rho) Y_J(\hat{\mathbf{r}}),$$

$$\mathcal{M}^A_J = \kappa^{-1} j_J(\rho) Y_J(\hat{\mathbf{r}})(\boldsymbol{\sigma}\cdot\boldsymbol{\nabla}),$$

$$\mathcal{M}^A_{MJ} = \sum_L i^{J-L-1} F_{MLJ}\, j_L(\rho)\left[Y_L(\hat{\mathbf{r}})\otimes\boldsymbol{\sigma}\right]_J,$$

$$\mathcal{M}^V_{MJ} = \kappa^{-1}\sum_L i^{J-L-1} F_{MLJ}\, j_L(\rho)\left[Y_L(\hat{\mathbf{r}})\otimes\boldsymbol{\nabla}\right]_J$$

Weak–nuclear interaction

$$
\begin{aligned}
\mathcal{T}_\sigma(\kappa, J_f) &= \frac{4\pi G^2}{2J_i+1}\sum_{\mathsf{J}}\Big[|\langle J_f||\mathsf{O}_{\emptyset \mathsf{J}}||J_i\rangle|^2\mathcal{L}_\emptyset + \sum_{\mathsf{M}=0,\pm 1}|\langle J_f||\mathsf{O}_{\mathsf{MJ}}||J_i\rangle|^2\mathcal{L}_{\mathsf{M}} \\
&- 2\Re(|\langle J_f||\mathsf{O}_{\emptyset \mathsf{J}}||J_i\rangle\langle J_f||\mathsf{O}_{0\mathsf{J}}||J_i\rangle)\mathcal{L}_{\emptyset 0}\Big] .
\end{aligned}
$$

☺ For natural parity states with $\pi=(-)^J$,i.e., 0^+, 1^-, 2^+, 3^-….

$$
\begin{aligned}
\mathsf{O}_{\emptyset \mathsf{J}} &= g_{\mathsf{V}}\mathcal{M}^V_{\mathsf{J}} \\
\mathsf{O}^{CVC}_{0\mathsf{J}} &= \frac{k_\emptyset}{\kappa} g_{\mathsf{V}}\mathcal{M}^V_{\mathsf{J}} \\
\mathsf{O}_{0\mathsf{J}} &= 2\overline{g}_{\mathsf{V}}\mathcal{M}^V_{0\mathsf{J}} - \overline{g}_{\mathsf{V}}\mathcal{M}^V_{\mathsf{J}} \\
\mathsf{O}_{\mathsf{M}\neq 0\mathsf{J}} &= (\mathsf{M}g_{\mathsf{A}} - \overline{g}_{\mathsf{W}})\hat{\mathcal{M}}^A_{1\mathsf{J}} + 2\overline{g}_{\mathsf{V}}\tilde{\mathcal{M}}^V_{1\mathsf{J}}
\end{aligned}
$$

☺ For unnatural parity states with $\pi=(-)^{J+1}$,i.e., 0^-, 1^+ ,2^-, 3^+….

$$
\begin{aligned}
-i\mathsf{O}_{\emptyset \mathsf{J}} &= 2\overline{g}_{\mathsf{A}}\mathcal{M}^A_{\mathsf{J}} + (\overline{g}_{\mathsf{A}} + \overline{g}_{\mathsf{P1}})\mathcal{M}^A_{0\mathsf{J}} \\
-i\mathsf{O}_{0\mathsf{J}} &= (\overline{g}_{\mathsf{P2}} - g_{\mathsf{A}})\mathcal{M}^A_{0\mathsf{J}} \\
-i\mathsf{O}_{\mathsf{M}\neq 0\mathsf{J}} &= (-g_{\mathsf{A}} + \mathsf{M}\overline{g}_{\mathsf{W}})\tilde{\mathcal{M}}^A_{1\mathsf{J}} + 2\mathsf{M}\overline{g}_{\mathsf{V}}\hat{\mathcal{M}}^V_{1\mathsf{J}}
\end{aligned}
$$

(i) deForest Jr.& Walecka, Adv.Phys15, 1(1966)

(ii) Kuramoto et al. NPA 512, 711 (1990)

(iii) Luyten et al. NP41,236 (1963)(μ-capture)

(iv) Krmpotic et al. PRC71, 044319(2005).

≈ all are equivalents.

$$
\mathsf{O}_{\emptyset \mathsf{J}} = \hat{\mathcal{M}}_{\mathsf{J}},
$$

$$
\mathsf{O}_{\mathsf{MJ}} = \begin{cases} \hat{\mathcal{L}}_{\mathsf{J}}, & \text{for} \quad \mathsf{M}=0 \\ -\frac{1}{\sqrt{2}}\left[\mathsf{M}\hat{\mathcal{T}}^{MAG}_{\mathsf{J}} + \hat{\mathcal{T}}^{EL}_{\mathsf{J}}\right], & \text{for} \quad \mathsf{M}=\pm 1 \end{cases}
$$

Nuclear Structure Models

(i) Models with **microscopical formalism** with detailed nuclear structure, solves the microscopic quantum-mechanical Schrodinger or Dirac equation, provides nuclear wave functions and (g.s.-shape E_{sp} , J^{π} , log (ft), $\tau_{1/2}$ ...) Examples:

Shell Model (Martinez et al. PRL83, 4502(1999))

RPA models

Self-Consistent Skyrme-HFB+QRPA

(Engel etal. PRC60, 014302(1999))

QRPA, Projected QRPA

(Krmpotic etal. PLB319(1993)393.)

Relativistic QRPA

(N. Paar et al., Phys. Rev. C 69, 054303 (2004))

Density Functional+Finite Fermi Syst.

(Borzov etal. PRC62, 035501 (2000))

(ii) Models describing **overall nucler properties** statistically where the parameters are adjusted to exp. data, no nuclear wave funct., polynomial or algebraic express.

Examples:

Fermi Gas Model,

Gross Theory of β-decay (GTBD)

Takahashi etal. PTP41,1470 (1969)

New exponential law for β^{+}.....

(Zhang etal. PRC73,014304(2006))

$\tau_{1/2}$ (Kar etal., astro-ph/06034517(2006))

Nuclear Structure Models

QRPA: Quasiparticle Random Phase Approximation

$$(e_t - \lambda_t)(u_t^2 - v_t^2) + u_t v_t \Delta_t = 0,$$

$$\begin{pmatrix} \mathcal{A} & \mathcal{B} \\ \mathcal{B} & \mathcal{A} \end{pmatrix} \begin{pmatrix} X \\ Y \end{pmatrix} = \omega \begin{pmatrix} X \\ -Y \end{pmatrix},$$

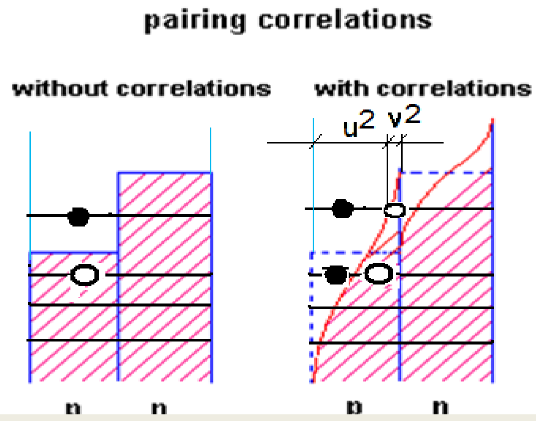

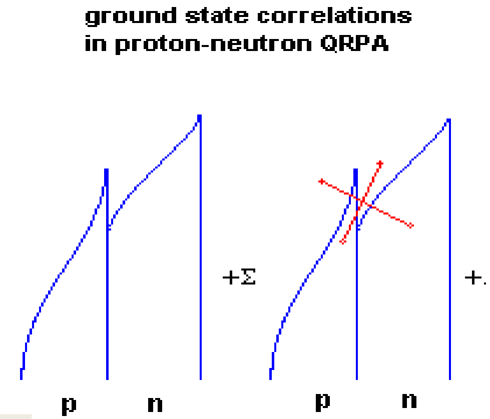

$$\langle BCS|\hat{N}|BCS\rangle \equiv \sum_{t=n(p)} (2j_t+1)v_{j_t}^2 = N(Z),$$

PQRPA: Projected QRPA

$$2\hat{e}_p u_p v_p - \Delta_p(u_p^2 - v_p^2) = 0,$$

$$\begin{pmatrix} \mathcal{A}_\mu & \mathcal{B} \\ -\mathcal{B}^\dagger & -\mathcal{A}^*_{-\mu} \end{pmatrix} \begin{pmatrix} \mathcal{X}_\mu \\ \mathcal{Y}_\mu \end{pmatrix} = \Omega_\mu \begin{pmatrix} \mathcal{X}_\mu \\ \mathcal{Y}_\mu \end{pmatrix},$$

Particle number is conserved exactly .

Krmpotic et al. PLB319(1993)393.

$$V = -4\pi\,(v_s P_s + v_t P_t)\,\delta(r),$$

Weak Observable Constrains

QRPA/PQRPA in ^{12}C

Gamow -Teller Strengths of Beta decay

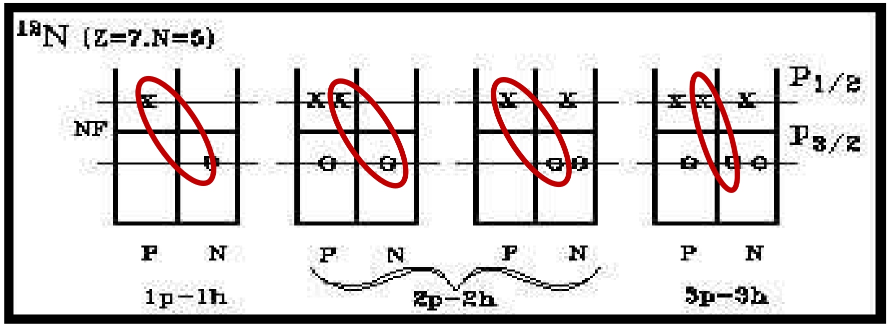

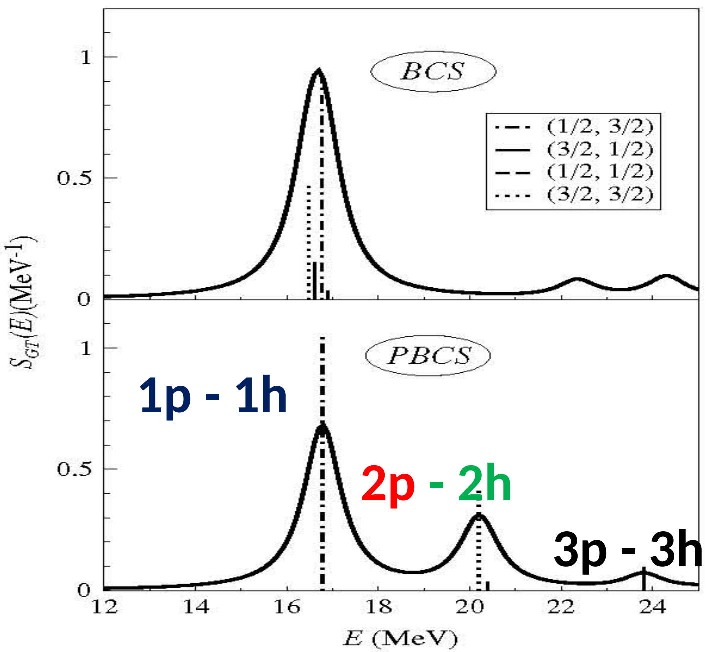

Volpe et al. PRC 62, 015501 (2000)``difficulties in choosing the g.s. of 12N because the lowest state is not the most collective one"

QRAP Quasiparticle RAndom Phase code

A. Samana, F. Krmpotic & C. Bertulani

Comp. Phys. Comm. 181 (2010)1123.

$$V = -4\pi \left(v_s P_s + v_t P_t \right) \delta(r),$$

PH-channel parameters from a systematic study GT resonances, F.K.&S.S. NPA 572, 329(1994)

P (I) : $v_s^{ph} = v^{pair}$, $v_t^{ph} = v_s^{ph}/0.6$

P(II): $v_s^{ph} = 27$, $v_t^{ph} = 64$

$$\left(v_s^{PP} \equiv v_s^{pair} \text{ and } v_t^{PP} \gtrsim v_s^{PP} \right)$$

$$t = \frac{2 v_t^{PP}}{v_s^{pair}(p) + v_s^{pair}(n)},$$

Neutrino/antineutrino cross sections ^{12}C

QRPA/PQRPA in ^{12}C

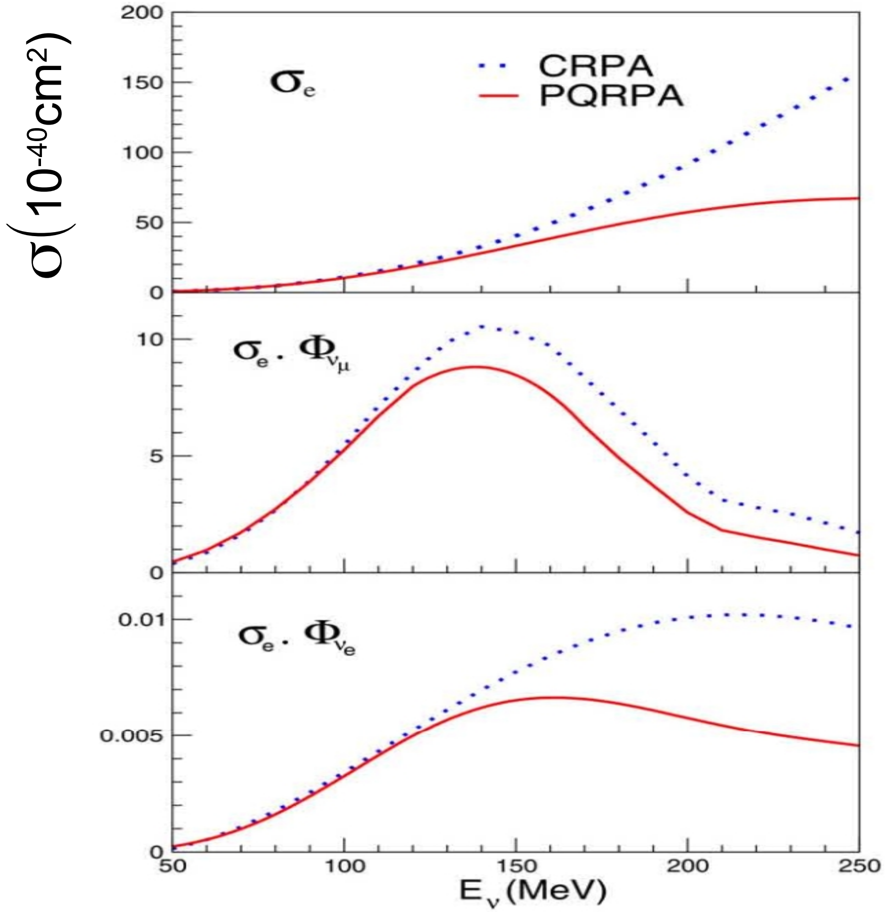

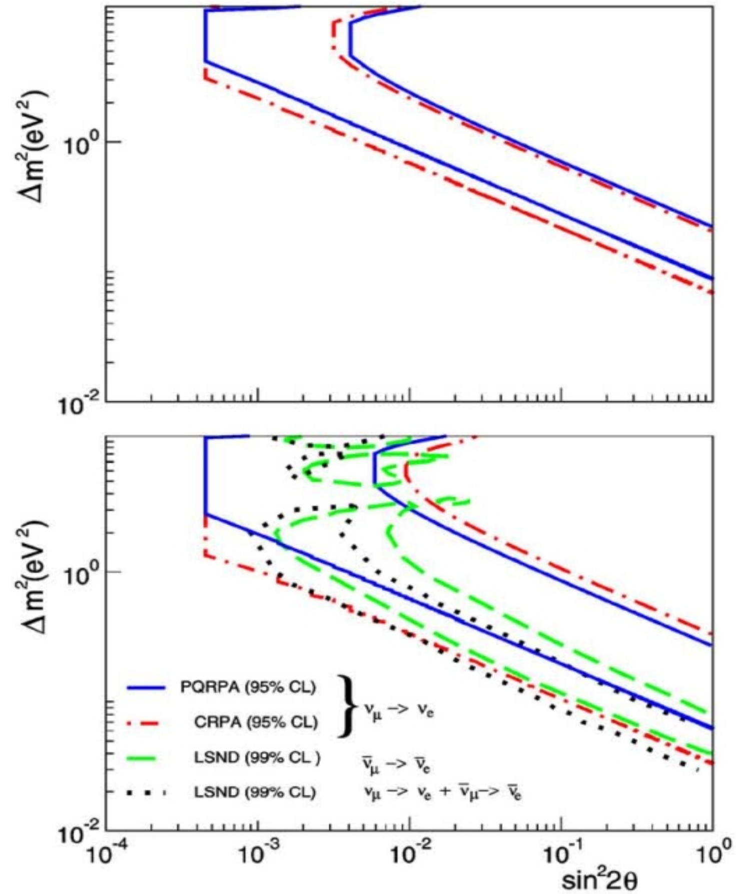

ν-nucleus cross section are important to constrain parameters in neutrino oscillations.

$\bar{\nu}_\mu \rightarrow \bar{\nu}_e \qquad \nu_\mu \rightarrow \nu_e$

* Increase probability oscillations.
* Confidence level region is diminished by difference in σ_e between PQRPA and CRPA,

A.Samana,et al.,PLB (2005) 100

Neutrino/antineutrino cross sections ^{56}Fe

QRPA/PQRPA in ^{56}Fe

Supernovae Neutrinos – To estimate events in supernova detectors.

$$N_e \equiv N_e(T_{\nu_e}) = N_t \int_0^{\infty} F_e^0(E_\nu, T_{\nu_e}) \sigma(E_\nu) \varepsilon(E_\nu) dE_\nu ,$$

$$\tilde{N}_e \equiv \tilde{N}_e(T_{\nu_x}) = N_t \int_0^{\infty} F_x^0(E_\nu, T_{\nu_x}) \sigma(E_\nu) \varepsilon(E_\nu) dE_\nu .$$

Effective temperature

Neutrino energy

Time-integrated energy

$$F_\alpha^0(E, T_\alpha, \eta_\alpha = 0, L_\alpha, D) = \frac{L_\alpha}{4\pi D^2 T_\alpha^4 F_3(0)} \frac{E^2}{e^{E/T_\alpha} + 1},$$

Distance to supernova

Norm.factor

Pinching parameter

D~ 10 kpc,

$L_\alpha = E_b \cdot 1/6$,

$E_b = 3 \times 10^{53}$ erg,

$\alpha = \nu_\alpha = \{\nu_e, \nu_\mu, \nu_\tau\}$

$T(\nu_x)/T(\underline{\nu}_e) = 1.5$,

$T(\nu_e)/T(\underline{\nu}_e) = 0.8$,

$T(\underline{\nu}_e) = 5$ MeV

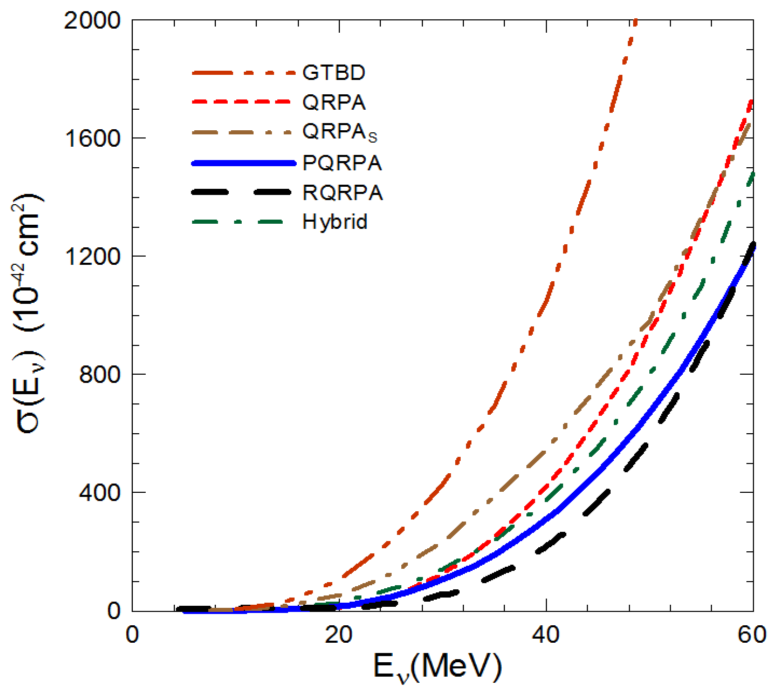

A. Samana & C. Bertulani, PRC 78, 024312 (2008)

Neutrino/antineutrino cross sections ^{56}Fe

A.S.& C.B., PRC 78, 024312 (2008)

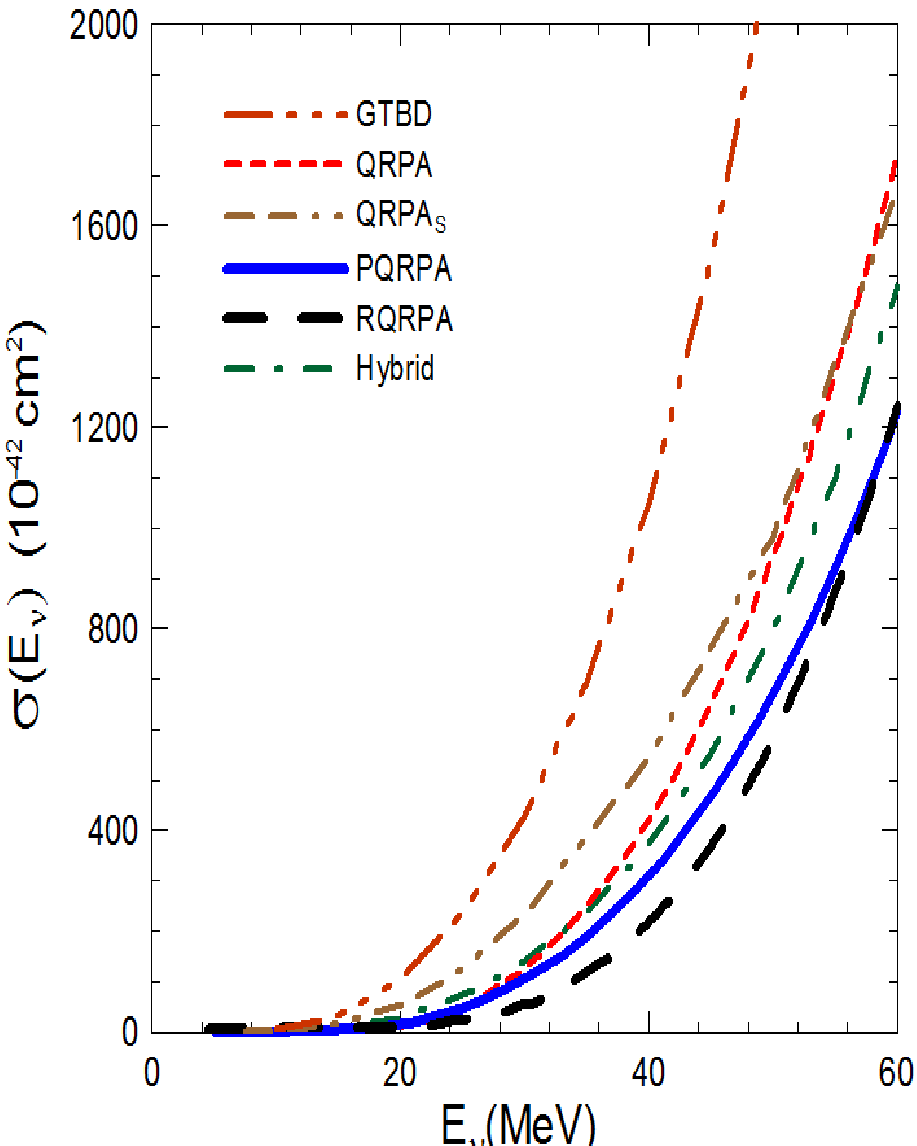

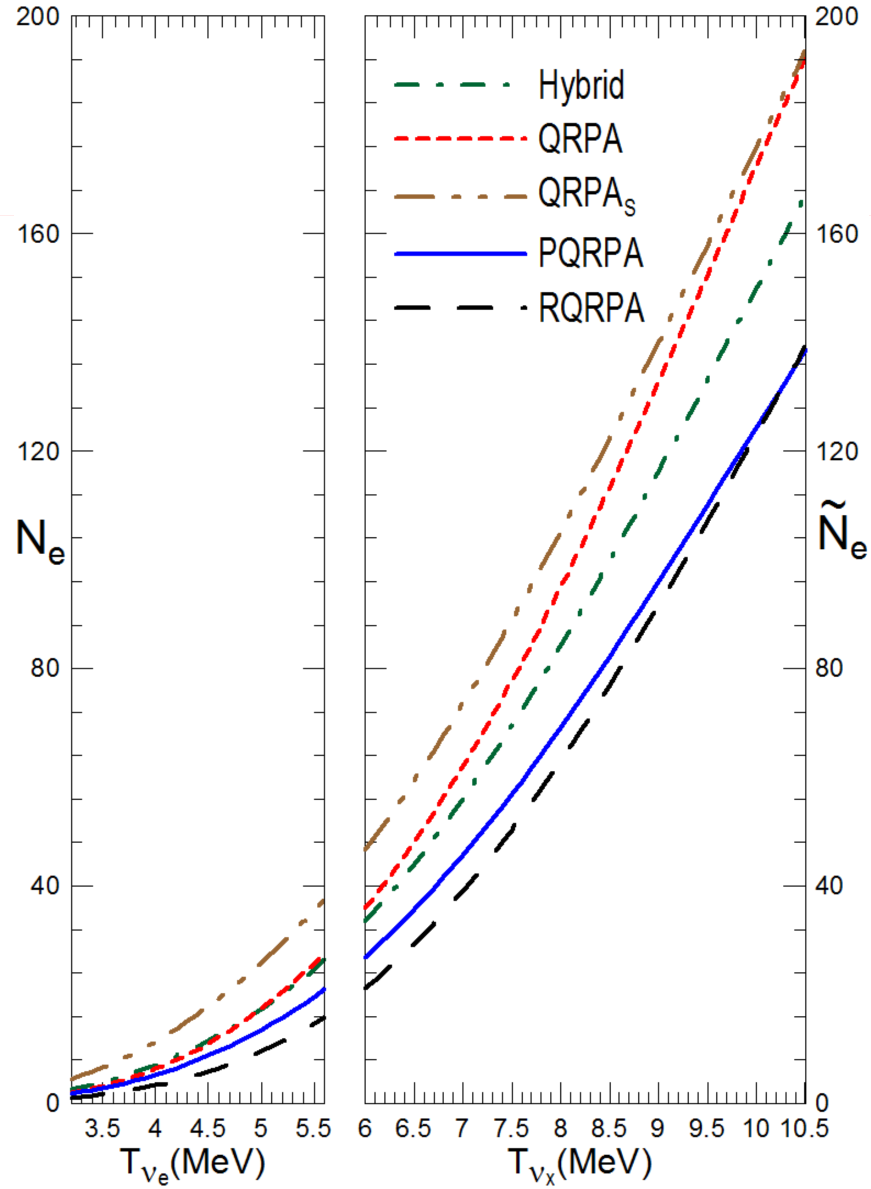

Neutrino/antineutrino cross sections ^{40}Ar

LArTPC - Liquid Argon Time Projection Chambers: ν_e-^{40}Ar

DUNE - Deep Underground Neutrino Experiment: ν_e - ^{40}Ar

- Some years ago G. McLaughlin talk me about to make a "gross averaged" of the CS for several nuclear models in ^{56}Fe. I disagree in that moment, nevertheless I change of idea due the difficult to obtain an error in the several theoretical nuclear models.
- In 40Ar, several work shown that:

- Gamow -Teller Strengths of Beta decay : low energy – GT resonances & IAS;
- Inclusive – exclusive muon capture rates: high energy - 100 MeV muon mass

RPA: Ormand,Pizzochero, Bortignon, Broglia, PLB 345(343)1995
RPA: Martinez-Pinedo, Kolbe & Langanke K, priv. comm. Gil-Botella & Rubbia, JCAP10 009 (2003)
SM : T. Suzuki & M. Honma, arXiv:1211.4078v1 [nucl-th] 17 Nov 2012
QRPA : M. Cheoun et al , PRC **83,** 028801 (2011).
QRPA & PQRPA: Samana et al. (2016).

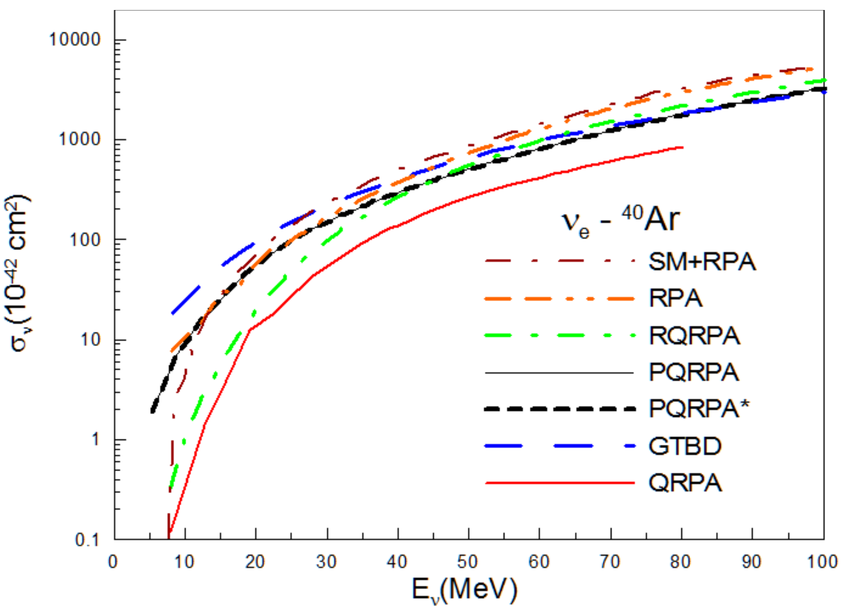

Supernovae Neutrinos – Signal Detection

SM + RPA (Suzuki & Honma)
PRC87, 014607(2013)

PQRPA

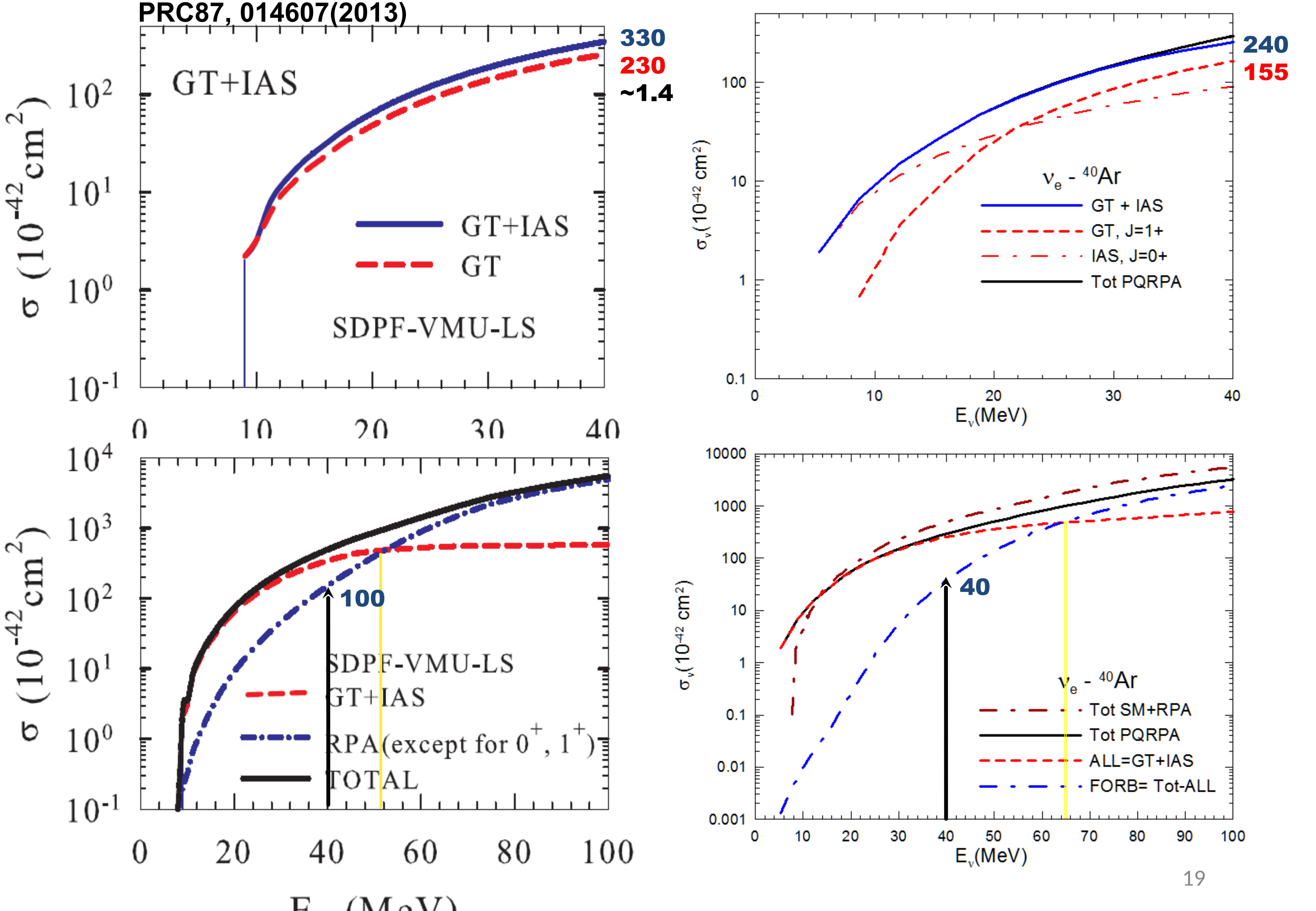

Neutrino/antineutrino cross sections ^{40}Ar

Folded cross section with SN fluxes

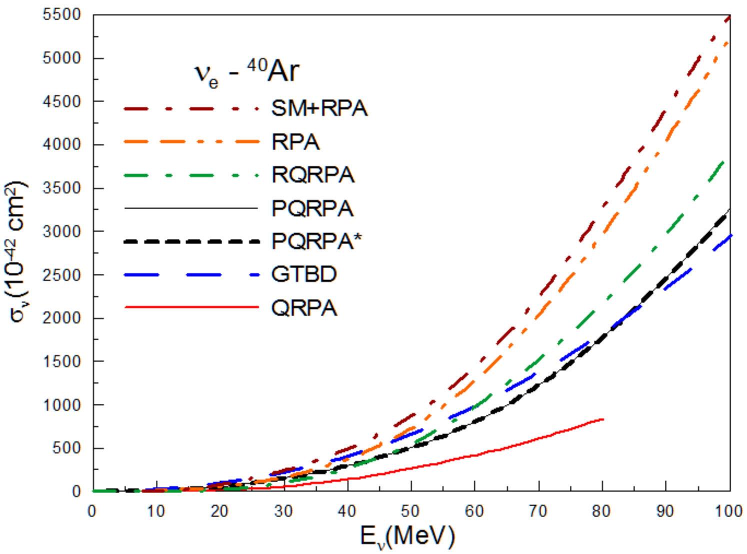

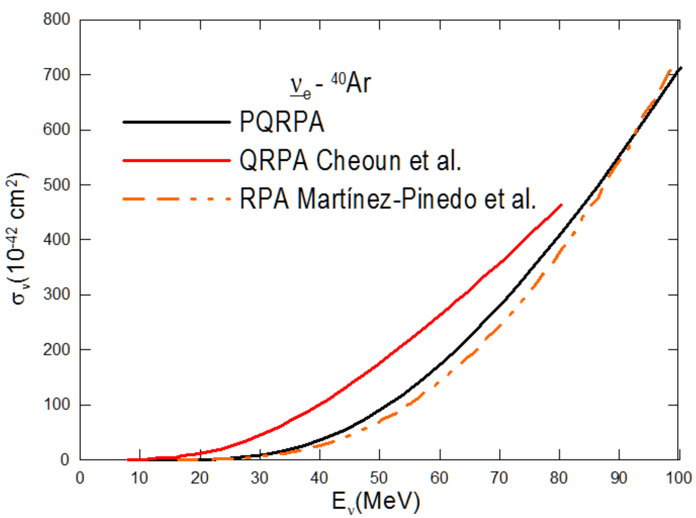

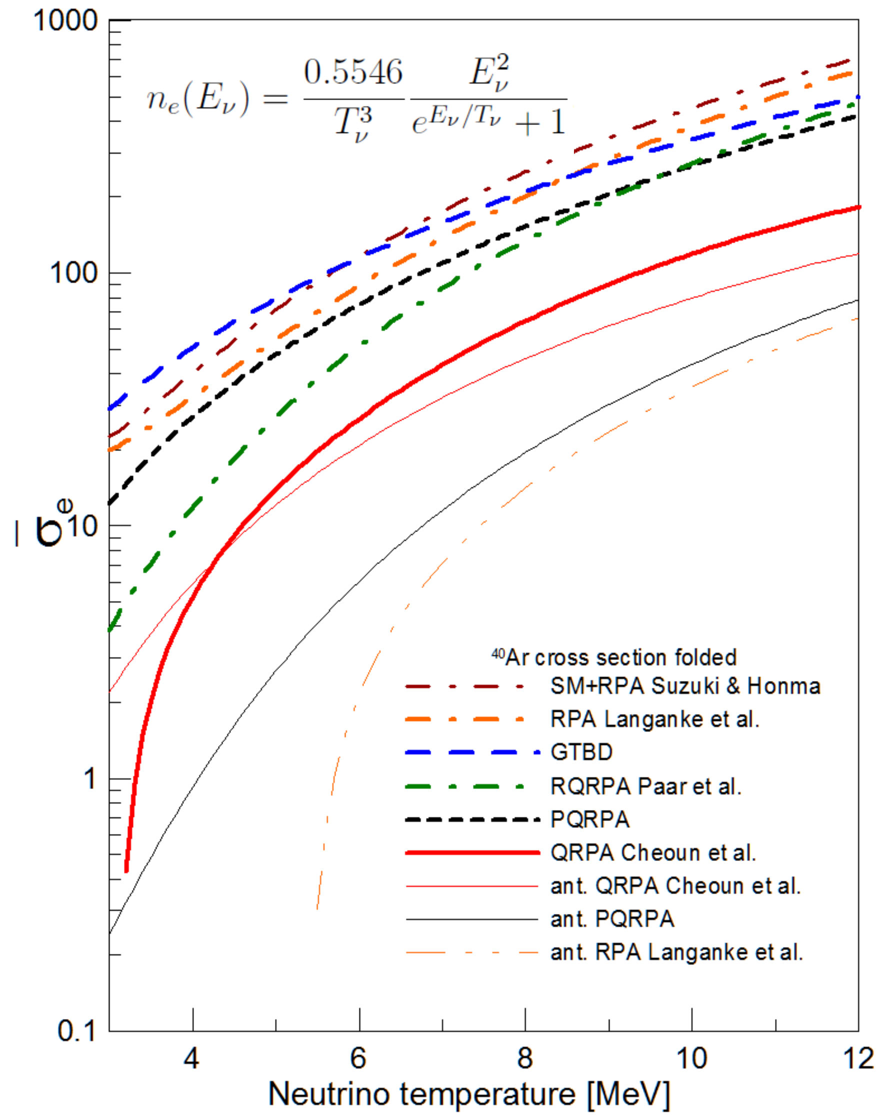

INSTITUTE for NUCLEAR THEORY

Neutrino/antineutrino cross sections ^{40}Ar

PHYSICAL REVIEW D 107, 112012 (2023)

Impact of cross-section uncertainties on supernova neutrino spectral parameter fitting in the Deep Underground Neutrino Experiment

- A key requirement for a correct interpretation of these measurements is a good understanding of the energy-dependent total cross section for charged-current neutrino electron absorption on argon.
- Using a toy model to neutrino spectra varying the cross section was found that large theoretical uncertainties on the cross section must be reduced before to extract the neutrino flux parameters.
- The neutrino spectral shape parameters can be known to better than 10% for a 20% uncertainty on the cross-section scale, although they will be sensitive to uncertainties on the shape of the CS,
- It is necessary to measure low- energy neutrino-Ar to improve theoretical precision,
- 12 cross section model were employed.

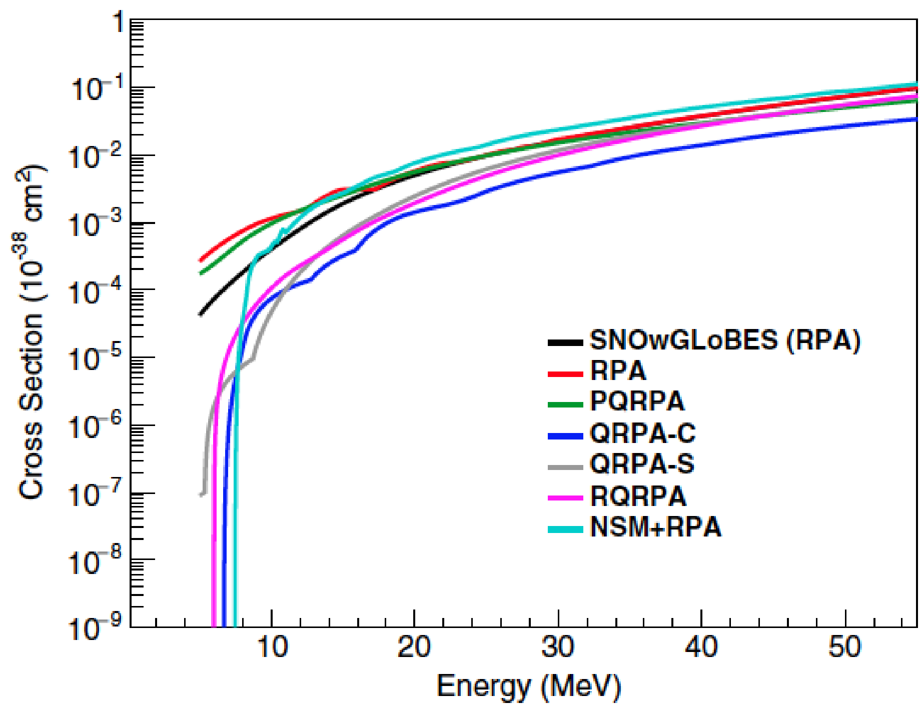

FIG. 6. Cross-section calculations for the $\nu_e - {}^{40}Ar$ interaction from Refs. [29,38–44]. The labels are explained in Table I. Note the log scale on the y-axis.

Neutrino/antineutrino cross sections ^{40}Ar

TABLE I. Brief features of $\nu_e - {}^{40}$Ar cross-section models used in this work.

Cross-section model	Model name	Comments
Default model implemented in SNOWGLOBES [29]	SNOWGLOBES or S	Based on RPA calculations for all multipole transitions up to $J^\pi = 4^\pm$.
Calculation by Martinez-Pinedo *et al.* [38,39]	RPA	Based on RPA calculations including all the multipole transitions up to $J^\pi = 6^\pm$.
Calculation by Cheoun *et al.* [43]	QRPA-C	Based on QRPA calculations. The results are consistent with data from (p, n) scattering reactions and Gamow-Teller strengths.
Calculation by Paar *et al.* [40]	RQRPA	Based on a self-consistent theory framework for a relativistic nuclear energy density functional. The cross sections are including higher-order multipole transitions up to $J^\pi = 5^\pm$. The calculations provide a larger cross sections for ^{40}Ar.
Calculation by Samana *et al.* [42]	PQRPA	Based on projected number QRPA including higher-order multipole transitions up to $J^\pi = 6^\pm$. These calculations were able to describe consistently the weak processes on ^{12}C [42] using a projection number particle procedure.
Calculation by Samana *et al.* [45,46]	GTBD	Based on the gross theory of beta decay, that describes global properties of β-decay processes. References [45,46] state that this model for heavy elements overestimated available data. Reference [16] states that GTBD is less reliable compared to (p, n) scattering data.
Calculation by Suzuki and Honma [41]	NSMRPA or NSM + RPA	Based on a hybrid-model calculation where partial cross sections for Fermi and Gamow-Teller transitions obtained using NSM, while other multipoles computed using RPA calculations.
MARLEY calculation based upon ^{40}Ti β decay data [32]	B 1998	Gamow-Teller matrix elements were extracted from a 1998 measurement by Bhattacharya *et al.* [47]. These are supplemented with QRPA matrix elements from Ref. [43] at high excitation energies.
MARLEY calculation based upon an alternative ^{40}Ti β decay data set [32]	L 1998	Gamow-Teller matrix elements were extracted from a 1998 measurement by Liu *et al.* [48]. These are supplemented with QRPA matrix elements from Ref. [43] at high excitation energies.
MARLEY calculation based upon (p, n) scattering data [32]	B 2009	Gamow-Teller matrix elements were extracted from a 2009 measurement by Bhattacharya *et al.* [49]. These are supplemented with QRPA matrix elements from Ref. [43] at high excitation energies.
Unpublished calculation by Samana and dos Santos [44]	QRPA-S	Based on QRPA calculations and using the same parametrization of present PQRPA, including higher-order multipole transitions up to $J^\pi = 6^\pm$.

INSTITUTE for NUCLEAR THEORY

Neutrino/antineutrino cross sections ^{40}Ar

(I) A ll of the microscopic models used here employ different residual interactions:
RPA - Skyrme interaction (including a spin-orbit term)
QRPA- Bonn CD potential
PQRPA- δ-interaction in PQRPA,
RQRPA- DDME2 relativistic nuclear energy density functional
SM - monopole based- universal interaction (VMU) in NSM + RPA.
The choice of was motivated by a successful description of: Gamow-Teller (GT) strengths, β-decay rates, muon capture rates.

$$\begin{pmatrix} \mathcal{A} & \mathcal{B} \\ \mathcal{B} & \mathcal{A} \end{pmatrix} \begin{pmatrix} X \\ Y \end{pmatrix} = \omega \begin{pmatrix} X \\ -Y \end{pmatrix}, \qquad (3.24)$$

where

$$\begin{aligned} \mathcal{A}(pnp'n';J) &= (E_p + E_n)\delta_{pp'}\delta_{nn'} \\ &\quad + (u_p v_n u_{p'} v_{n'} + v_p u_n v_{p'} u_{n'}) F(pnp'n';J) \\ &\quad + (u_p u_n u_{p'} u_{n'} + v_p v_n v_{p'} v_{n'}) G(pnp'n';J), \\ \mathcal{B}(pnp'n';J) &= (v_p u_n u_{p'} v_{n'} + u_p v_n v_{p'} u_{n'}) F(pnp'n';J) \\ &\quad + (u_p u_n v_{p'} v_{n'} + v_p v_n u_{p'} u_{n'}) G(pnp'n';J). \end{aligned} \qquad (3.25)$$

$$\begin{aligned} &\langle J_f, Z+\mu, N-\mu \| \mathrm{O}_J \| 0^+ \rangle \\ &= \sum_{pn} [\Lambda_\mu(pnJ) X^*(pnJ_f) + \Lambda_{-\mu}(pnJ) Y^*(pnJ_f)], \end{aligned}$$

$$\Lambda_\mu(pnJ) = -\frac{\langle p \| \mathrm{O}_J \| n \rangle}{\sqrt{2J+1}} \begin{cases} u_p v_n, & \text{for } \mu = +1, \\ u_n v_p, & \text{for } \mu = -1, \end{cases}$$

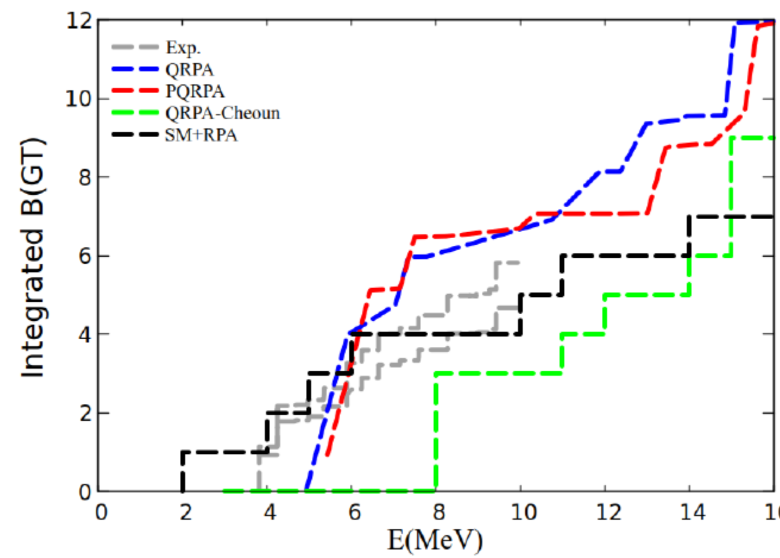

Fig. 5: Comparison of cumulative sum of the Gamow-Teller Strength B(GT) for QRPA (blue) and PQRPA (red), with experimental data (gray) [38], QRPA using Bonn-potential (green) [6] and Shell model+RPA (black) [2].

Samana et al,
CPC 181 (2010) 1123

$$\frac{|g_A \langle J_f \| \sigma \| J_i \rangle|^2}{2J_i + 1} \equiv B(\mathrm{GT}) = \frac{6146}{ft}\ \mathrm{s}.$$

INSTITUTE for NUCLEAR THEORY

Neutrino/antineutrino cross sections ^{40}Ar

(II) Second, using a sufficiently large configuration space of nucleon states is important to prevent underestimation of the energy-dependent total cross section $\sigma(E_\nu)$ as the neutrino energy rises.

$$\sigma(E_\nu) = \sigma(E_\nu, 0^+) + \sigma(E_\nu, 1^+) + \sigma(E_\nu, 0^-) + \sigma(E_\nu, 1^-) + \sum_{J^\pi \geq 2^\pm}^{8^\pm} \sigma(E_\nu, J^\pi) .$$

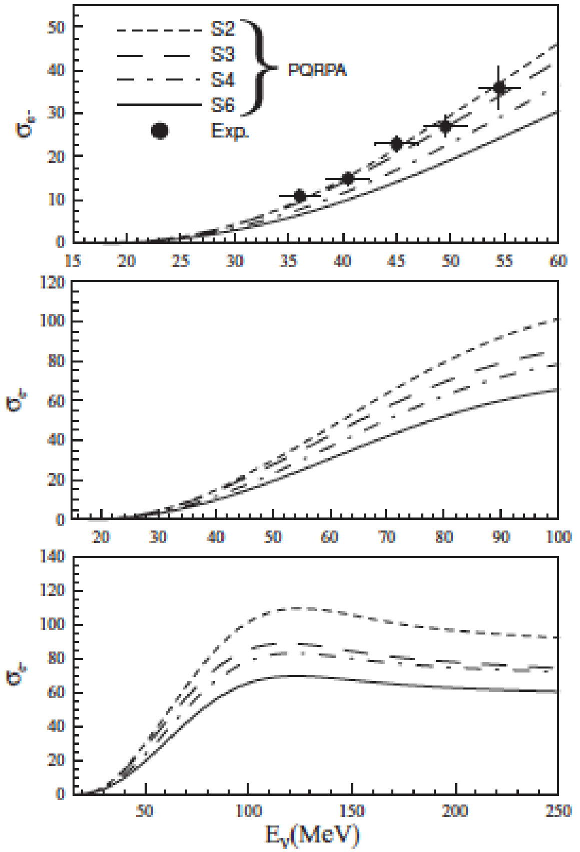

FIG. 2. Exclusive $^{12}C(\nu, e^-)^{12}N$ cross section $\sigma_e(E_\nu, 1^+_1)$ (in units of 10^{-42} cm^2), plotted as a function of the incident neutrino energy

Samana, Krmpotic, Paar, Bertulani
PRC 83, 024303 (2011)

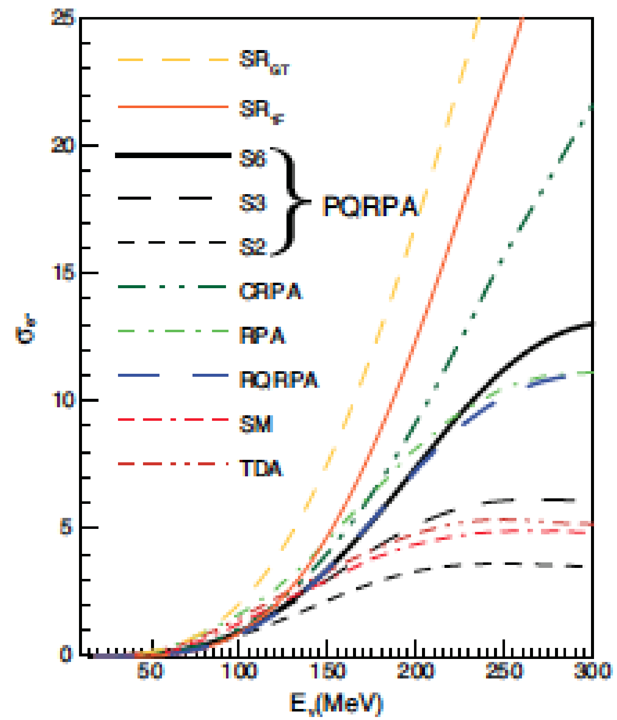

FIG. 6. (Color online) Inclusive $^{12}C(\nu, e^-)^{12}N$ cross section $\sigma_{e^-}(E_\nu)$ (in units of 10^{-39} cm^2) plotted as a function of the incident neutrino energy E_ν. PQRPA results within s.p. spaces S_2, S_3, and

Neutrino/antineutrino cross sections ^{40}Ar

(II) Second, using a sufficiently large configuration space of nucleon states is important to prevent underestimation of the energy-dependent total cross section $\sigma(E_\nu)$ as the neutrino energy rises.

$$\sigma(E_\nu) = \sigma(E_\nu, 0^+) + \sigma(E_\nu, 1^+) + \sigma(E_\nu, 0^-) + \sigma(E_\nu, 1^-) + \sum_{J^\pi \geq 2^\pm}^{8^\pm} \sigma(E_\nu, J^\pi) .$$

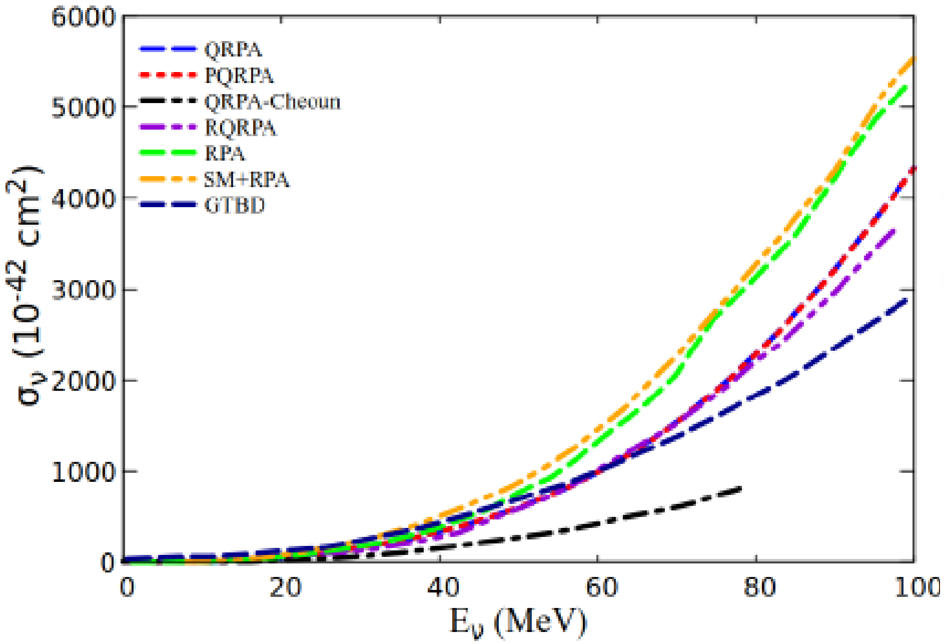

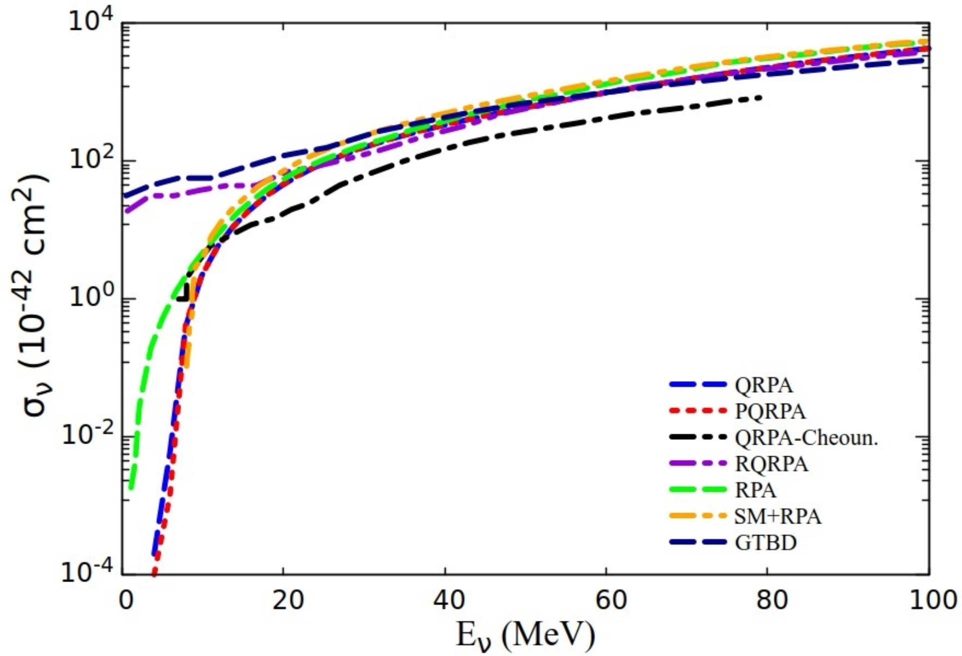

PQRPA and QRPA, RPA [Gil-Botella & Rubia, 2003], SM+RPA[Suzuki & Honma, 2013], GTBD [Samana et al, 2022], RQRPA [Paar et al., 20] and QRPA with Bonn potencial [Cheon et. al, 2011].

Neutrino/antineutrino cross sections ^{40}Ar

(III) some calculations use an effective (or quenched) value of the nucleon axial-vector coupling constant for which its bare value g_A=1.2756 from the experimental data is multiplied by a factor of around 0.8. There is still a lack of consensus in the nuclear physics community about whether this quenching is needed: fq=$g_{A,eff}$ /g_A

PQRPA and QRPA	$g_{A,eff}$=1.0	fq=0.784
RPA [Gil-Botella & Rubia, 2003]	$g_{A,eff}$=1.27	fq=1.0
RPA [Kolbe, 2003].................	$g_{A,eff}$=1.27	fq=1.0
SM+RPA[Suzuki & Honma, 2013].........................	$g_{A,eff}$=0.98	fq=0.775
GTBD [Samana et al, 2022]	$g_{A,eff}$=1.0	fq=0.784
RQRPA [Paar et al., 20]	$g_{A,eff}$=1.0	fq=0.784
QRPA with Bonn potencial [Cheon et. al, 2011].......	$g_{A,eff}$=0.94	fq=0.74

Most of these model adopt $g_{A,eff}$ to reproduce GT strength or cumulative sum of the GT strength.

Neutrino/antineutrino cross sections ^{40}Ar

PRD107, 112012 (2023)

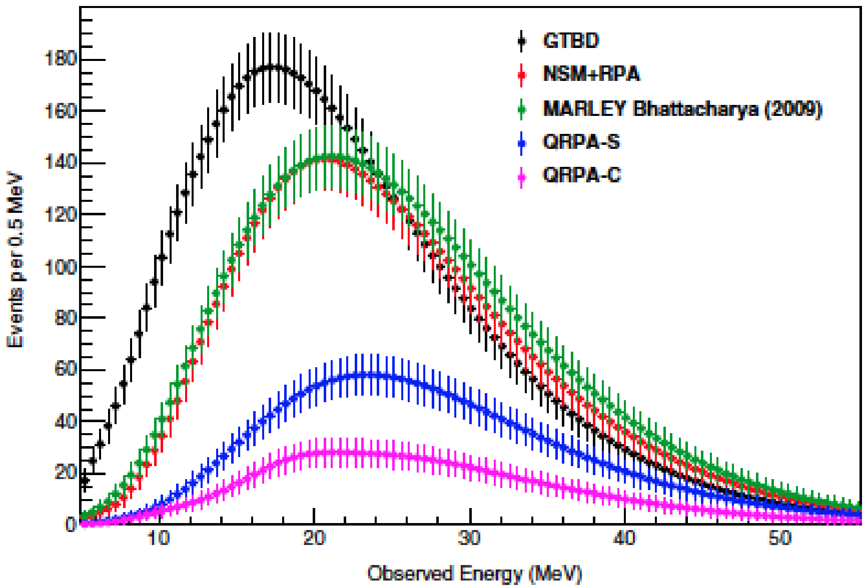

FIG. 8. SNOWGLOBES event rates for select cross-section calculations from Refs. [31,41,43–46]. The initial fluence parameter values for ν_e are $(\alpha^0, \langle E_\nu \rangle^0, \epsilon^0) = (2.5, 9.5\ \text{MeV}, 5\times 10^{52}\ \text{ergs})$, for $\bar{\nu}_e$ are $(\alpha^0, \langle E_\nu \rangle^0, \epsilon^0) = (2.5, 12.0\ \text{MeV}, 5\times 10^{52}\ \text{ergs})$, and for ν_x are $(\alpha^0, \langle E_\nu \rangle^0, \epsilon^0) = (2.5, 15.6\ \text{MeV}, 5\times 10^{52}\ \text{ergs})$. Normal mass ordering and MSW resonance were assumed. Note that "QRPA-C" and "QRPA-S" contain the same type of calculation performed by different groups, with the former by Cheoun *et al.* [43] and the latter by Samana and dos Santos [44]. More details about the various models are provided in Table I. The error bars are statistical.

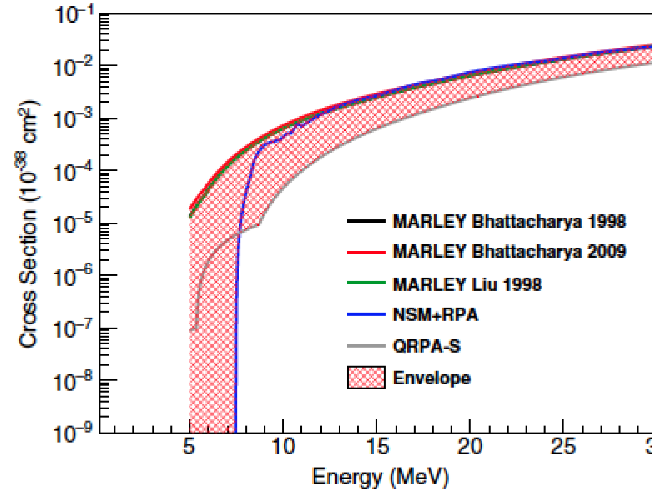

FIG. 15. Total cross section predictions for the $\nu_e - {}^{40}$Ar interaction from the selected subset of models discussed in Sec. III D. The shaded region represents the adopted uncertainty envelope based on the spread of these models.

TABLE IV. SNOWGLOBES estimated number of ν_eCC events in the DUNE far detectors for pinched-thermal flux parameters $(\alpha, \langle E_\nu \rangle, \epsilon) = (2.5, 9.5, 5\times 10^{52})$ for the ν_e flavor, a 10 kpc supernova, and assuming NMO and MSW oscillations via Eq. (5).

Cross-section model	Number of ν_eCC events	Number of ν_eCC events between [5, 15] MeV
QRPA-C [43]	1383	134
RQRPA [40]	2243	220
QRPA-S [44]	2791	243
SNOWGLOBES [29]	4486	624
B 1998 [32]	6307	874
L 1998 [32]	6390	883
NSM + RPA [41]	6391	897
B 2009 [32]	6852	988
PQRPA [42]	4562	909
RPA [38,39]	5064	998
GTBD [45,46]	7770	2070

INSTITUTE for NUCLEAR THEORY

Neutrino/antineutrino cross sections ^{40}Ar

QRPA/PQRPA in ^{40}Ar – Weak observables constrains

- Gamow -Teller Strengths of Beta decay : low energy – GT resonances & IAS
- Inclusive – exclusive muon capture rates: high energy - 100 MeV muon mass

Fermi strength and energy to fix ‘s’ isovector pp.

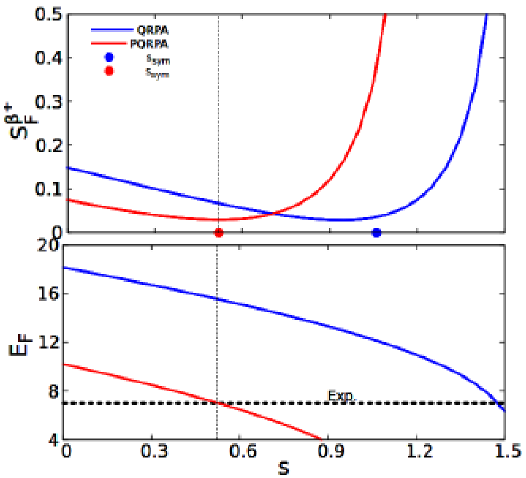

GT strength and energy to fix ‘t’ isovector pp.

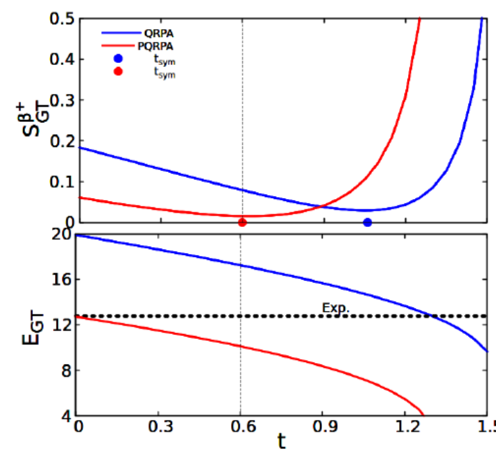

Muon capture rate distribution.

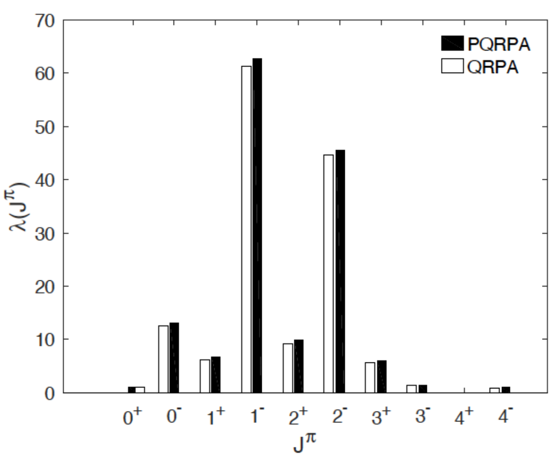

Experimental Muon caoture rate

120×10^3 /s

PQRPA

147.3×10^3 /s

QRPA

142.7×10^3 /s

Cumulative sum of the GT strength for 40Ar → 40K

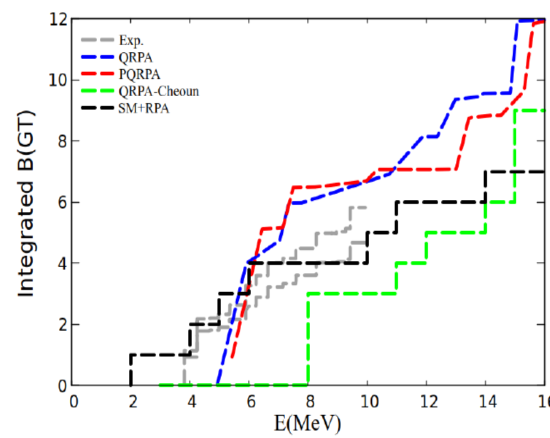

INSTITUTE for NUCLEAR THEORY

Neutrino/antineutrino cross sections ^{40}Ar

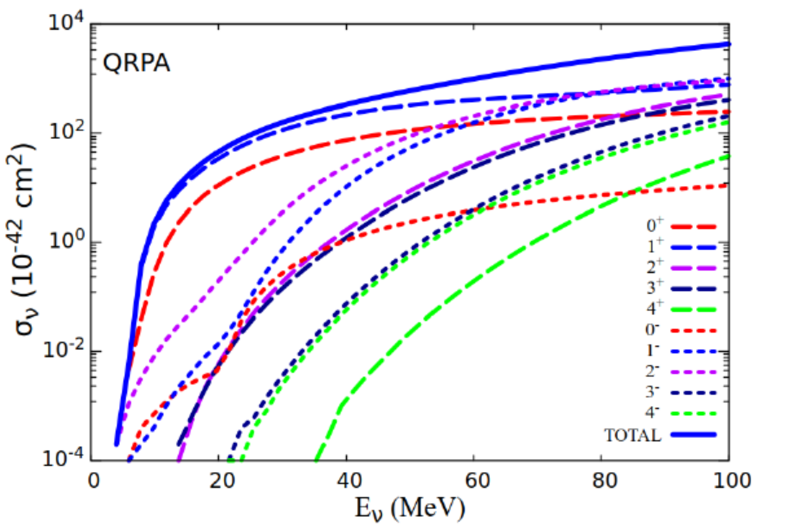

Fig. 10: Partial cross section for the reaction $(\nu_e, {}^{40}\mathrm{Ar})$ for the main multipole states contribution $J^\pi = 0^\pm - 4^\pm$, obtained using QRPA model.

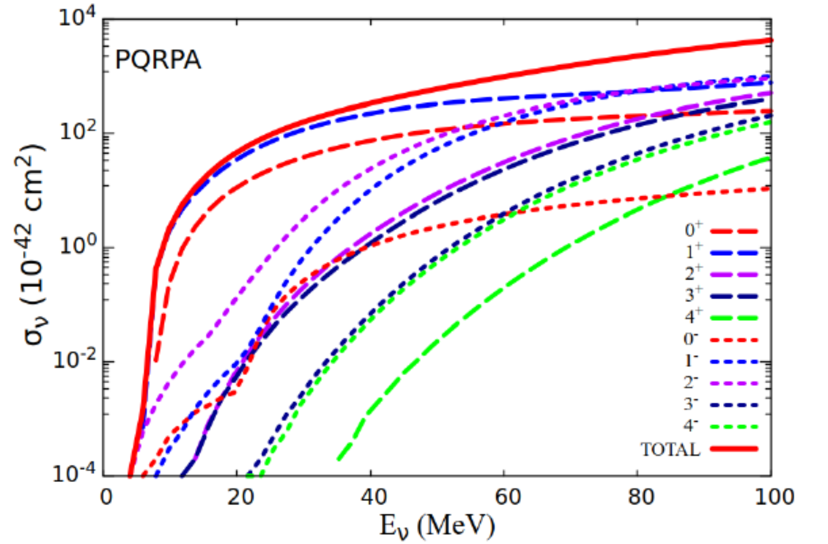

Fig. 11: Partial cross section for the reaction $(\nu_e, {}^{40}\mathrm{Ar})$ for the main multipole states contribution $J^\pi = 0^\pm - 4^\pm$, obtained using PQRPA model.

Allowed and forbidden contribution for PQRPA.

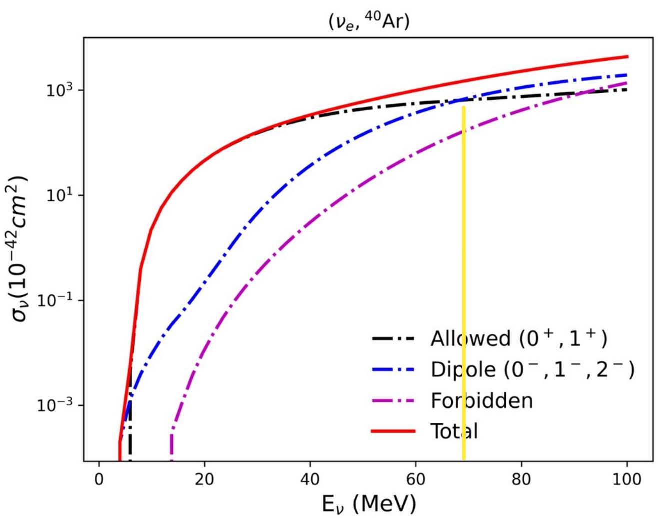

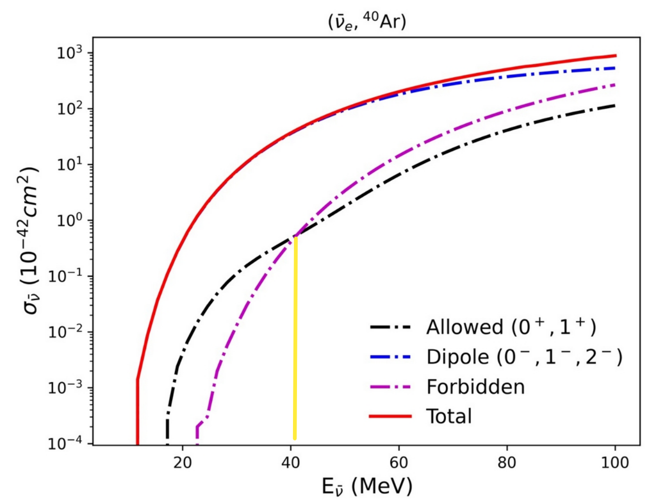

INSTITUTE for NUCLEAR THEORY

Neutrino and antineutrino cross section in 18O and 40Ar within QRPA models -INT-23-2– Seattle- USA - 2023

Neutrino/antineutrino cross sections ^{40}Ar

Averaged ν_e -40Ar cross section with Michel spectrum, neutrinos from muon decay.

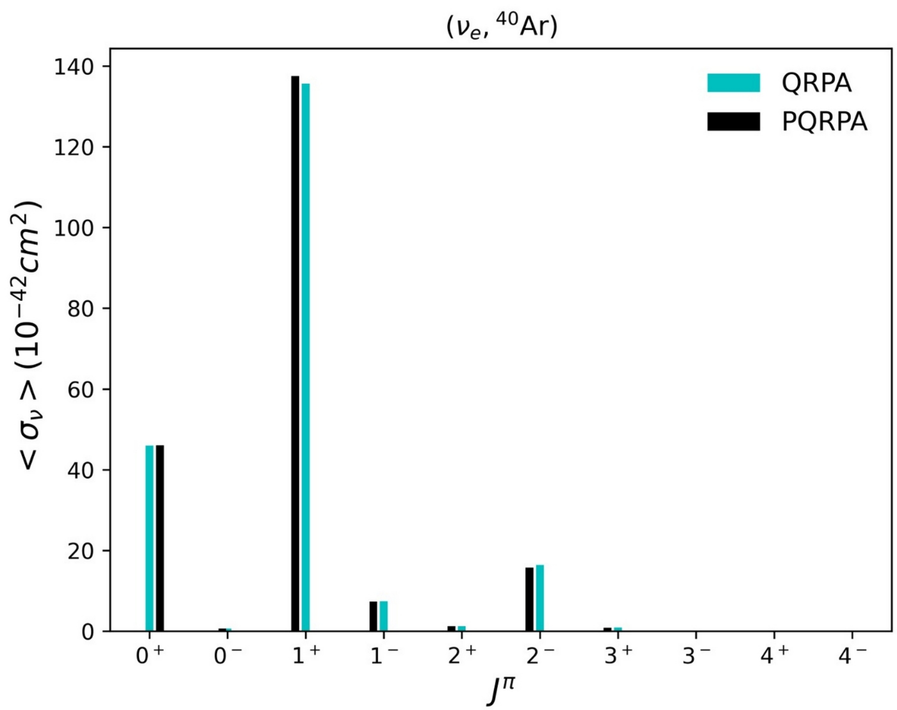

Neutral ν_e -40Ar cross section as function of neutrino energy.

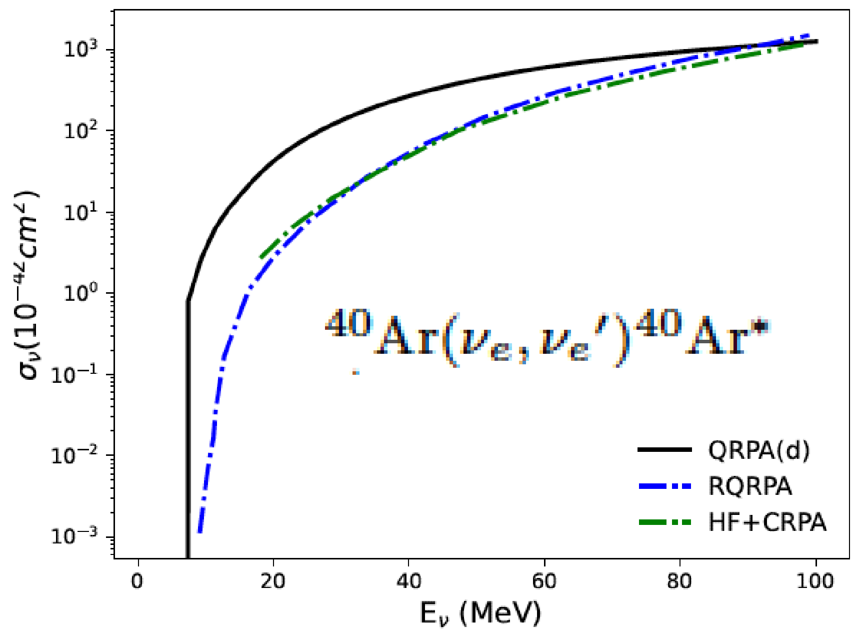

Main contributions come from allowed transitions.

$$\langle\sigma\rangle \equiv \frac{\int_0^{m_\mu/2} \sigma(E_\nu)\phi(E_\nu)dE_\nu}{\int_0^{m_\mu/2} \phi(E_\nu)dE_\nu}, \qquad \phi(E_\nu) \propto E_\nu^2 m_\mu^{-4}(m_\mu - 2E_\nu).$$

INSTITUTE for NUCLEAR THEORY

Neutrino/antineutrino cross sections on ^{18}O

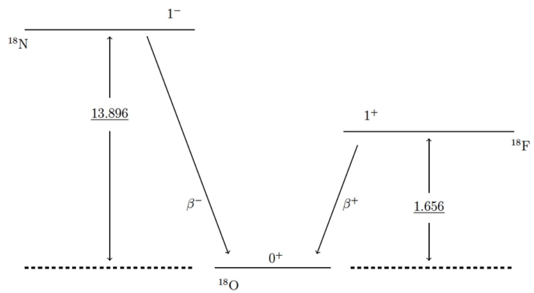

spe energies from DDME2

Shell	e_j^N	e_j^Z
$1s_{1/2}$	-43.54	-42.16
$1p_{3/2}$	-22.63	-22.20
$1p_{1/2}$	-16.33	-15.90
$1d_{5/2}$	-5.15	-5.11
$2s_{1/2}$	-2.57	-2.27
$1d_{3/2}$	-2.31	1.36
v_s^{pair}	15.40	27.82
Δ_{exp}	2.04	3.97
Δ_{th}	2.04	3.98

ph-channel

- ph1: $v_s^{\text{ph}} = 10.00,\ v_t^{\text{ph}} = vs^{\text{ph}}/0.6 = 16$
- ph2: $v_s^{\text{ph}} = 27.00,\ v_t^{\text{ph}} = 64.00.$

pp-channel

$$t = \frac{v_t^{\text{pp}}}{v_s^{\text{pair}}}\ ,\ s = \frac{v_s^{\text{pp}}}{v_s^{\text{pair}}}.$$

Nuclear interaction: delta force

$$V = -4\pi(v_t P_t + v_s P_s)\delta(r),$$

Pairing channel: v_s^{pairN} v_s^{pairZ}

$$\Delta^N = \frac{1}{2}\left[2B(Z,N) - B(Z,N-1) - B(Z,N+1)\right],$$

$$\Delta^Z = \frac{1}{2}\left[2B(Z,N) - B(Z-1,N) - B(Z+1,N)\right],$$

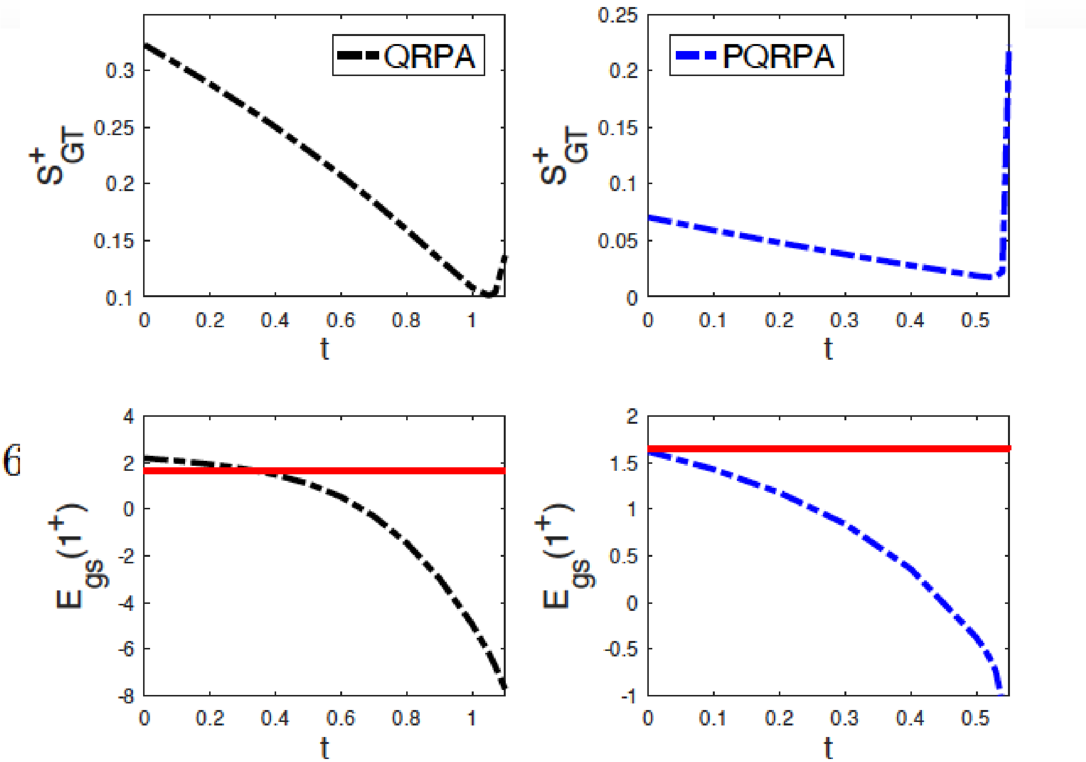

Neutrino/antineutrino cross sections on ^{18}O

(a) QRPA with t = 0 and s = 0.5 in the pp-channel and ph1 in the ph-channel;

(b) PQRPA with t = 0 and s = 0.5 in the pp-channel and ph1 in the ph-channel;

(c) QRPA with t = 0 and s = 0.5 in the pp-channel and ph2 in the ph-channel;

(d) QRPA with t = 0 and s = 1.0 in the pp-channel and ph1 in the ph-channel.

Inclusive muon capture rate

s		Model/t	0.0	0.2	0.35	0.4
0.5	ph1	QRPA (a)	85.97	84.69	84.32	84.45
0.5	ph1	PQRPA(b)	78.37	77.16	76.83	76.69
0.5	ph2	QRPA (c)	64.43	64.16	63.83	63.69
1	ph1	QRPA (d)	83.51	83.15	82.75	82.58
	λ_{inc}^{exp}		88 ± 1.5			

s=0.5 and t = 0.2 for PQRPA.

s=0.5 and t = 0.35 for QRPA.

Neutrino and Antineutrino captures on 18O within QRPA models,Mohammadzadeh, Khalili, Samana, dos Santos, Barbero and Duarte,
Eur. Phys. J. A (2023) 59:31

B(GT) for 18F, green t=0.2, blue t=0.4

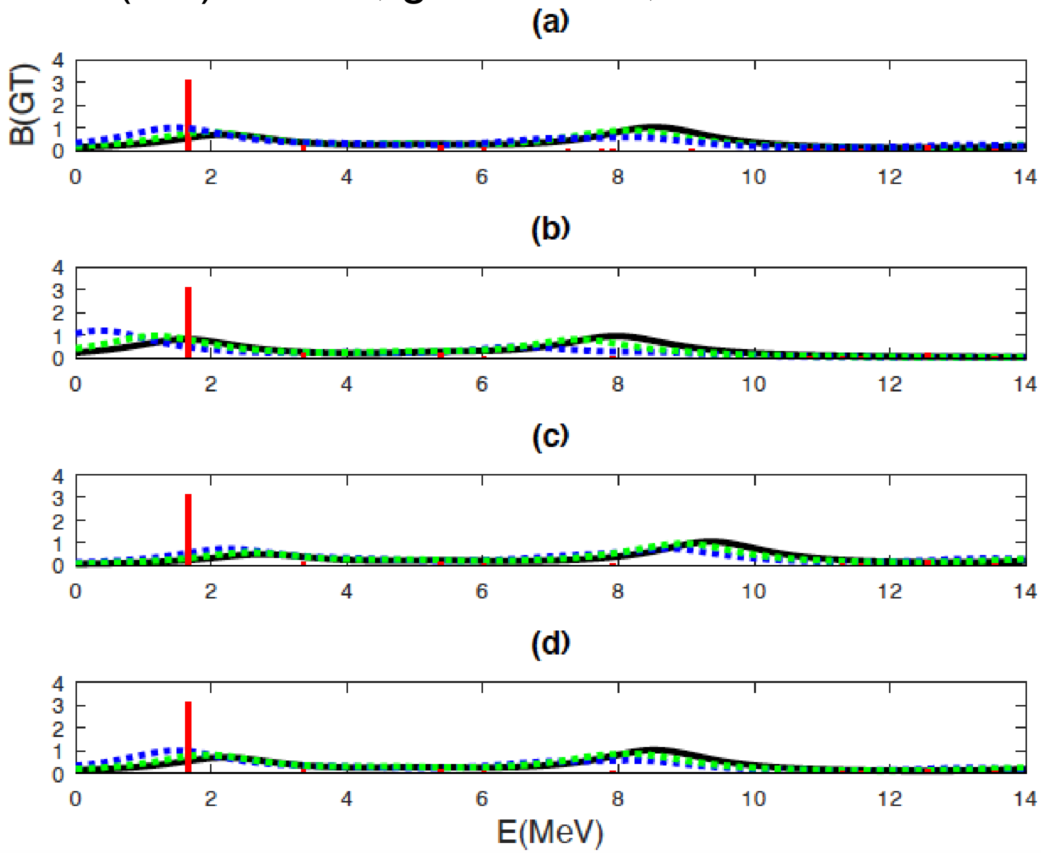

Neutrino/antineutrino cross sections on ^{18}O

Inclusive muon capture rate for ph1 and s=0.5 and t = 0.2 for PQRPA,s=0.5 and t = 0.35 for QRPA.

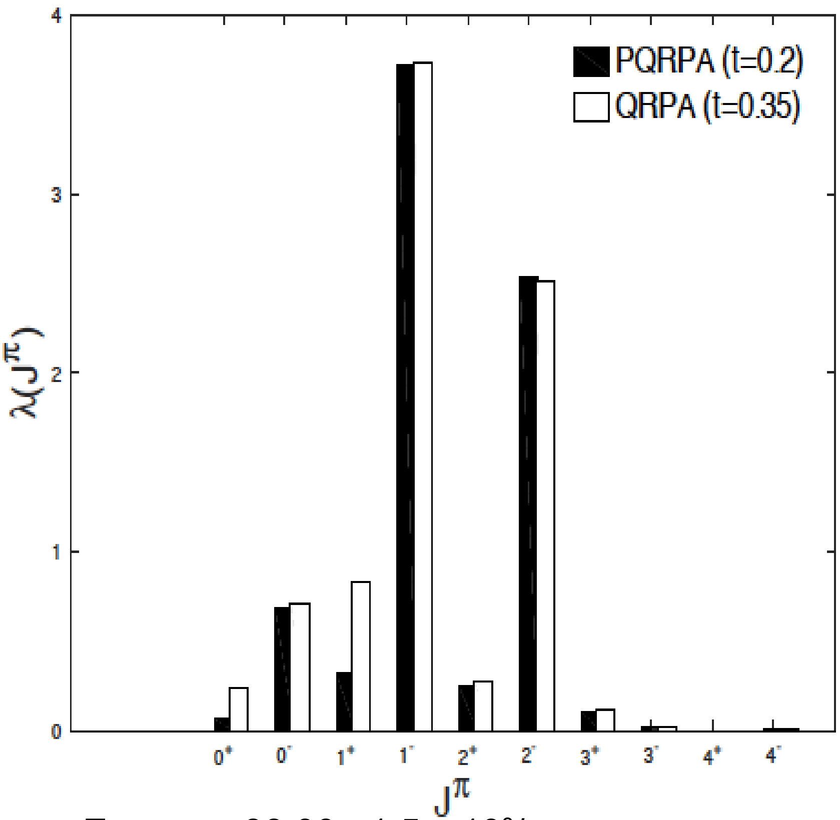

Exp= 88.00 ±1.5 x 10^3/s
QRPA= 84.32 x 10^3/s
PQRPA= 77.16 x 10^3/s

$\nu_e(^{18}O, ^{18}F_{gs}(1^+_1))e^-$

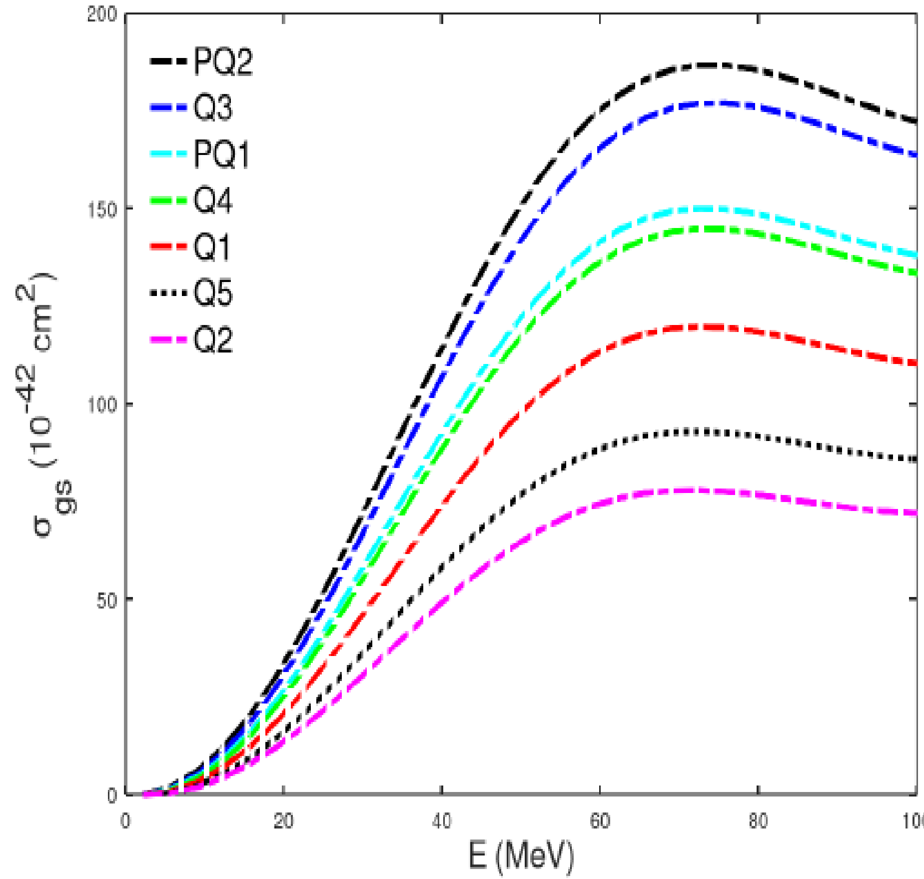

Exclusive CS for Q1 (a), PQ1 (b), Q2 (c) with t = 0.0, Q3 (a) with t = 0.35, PQ2 (b), Q4 (a) and Q5 (c) with t = 0.2.

Neutrino/antineutrino cross sections on ^{18}O

Neutrino-18O CS for PQRPA(t=0,2 & ph1) and QRPA (t=0,35 & ph1).

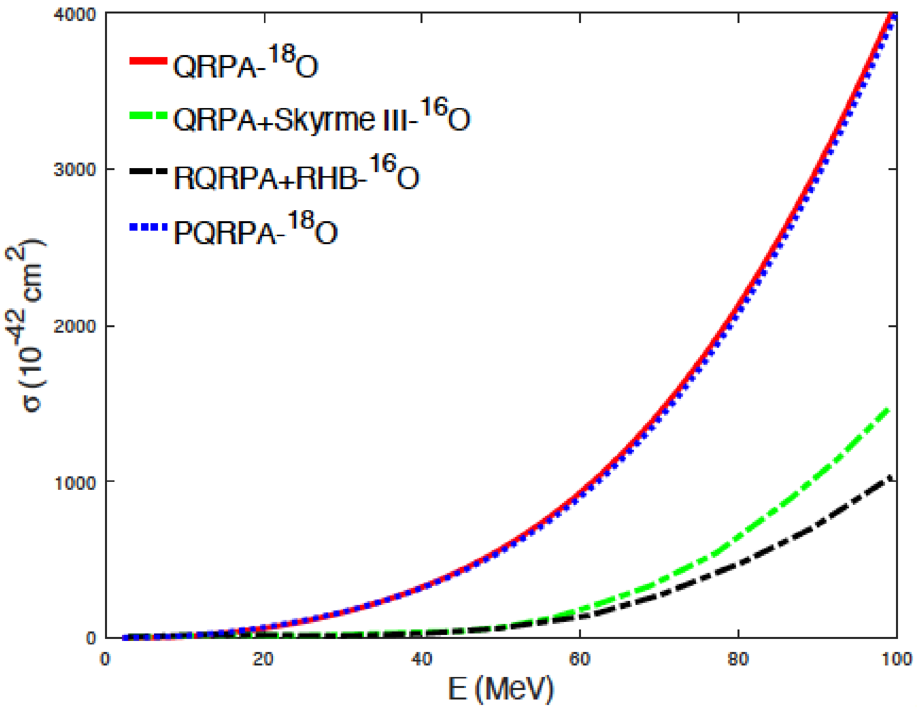

Anti-neutrino-18O CS for PQRPA(t=0,2 & ph1) and QRPA (t=0,35 & ph1).

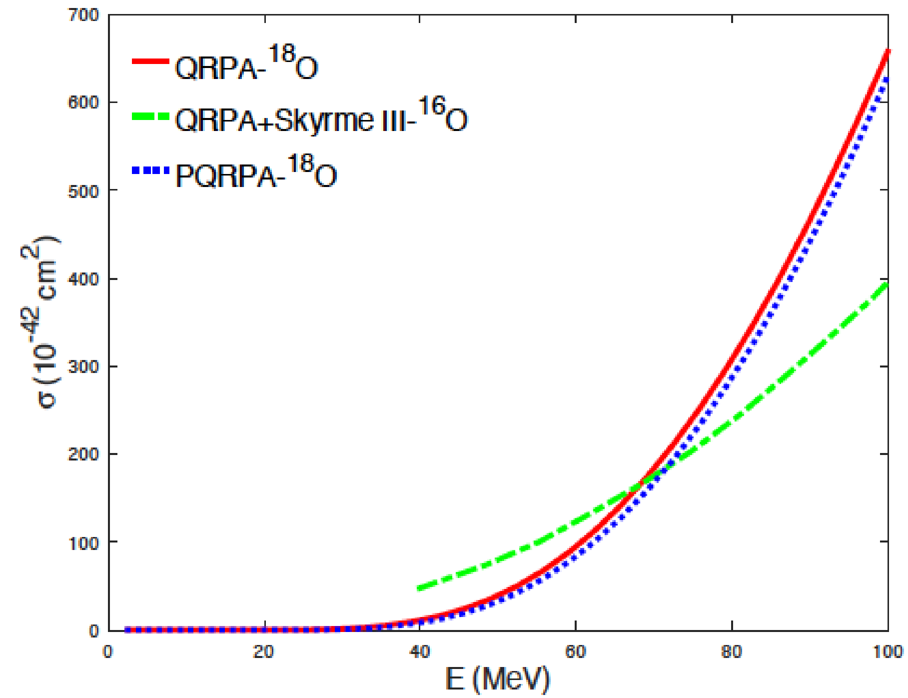

Neutrino/antineutrino cross sections on ^{18}O

Neutrino-18O CS for PQRPA(t=0.2 & ph1)

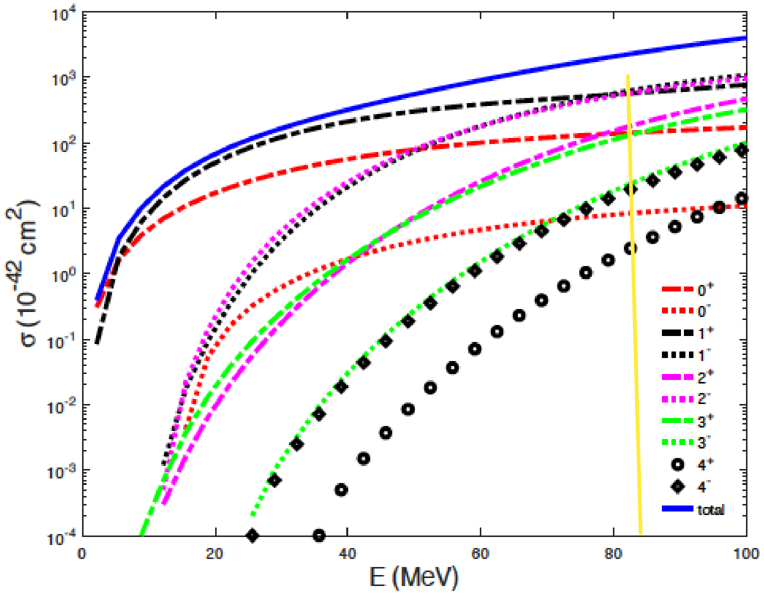

Anti-neutrino-18O CS for PQRPA(t=0.2 & ph1)

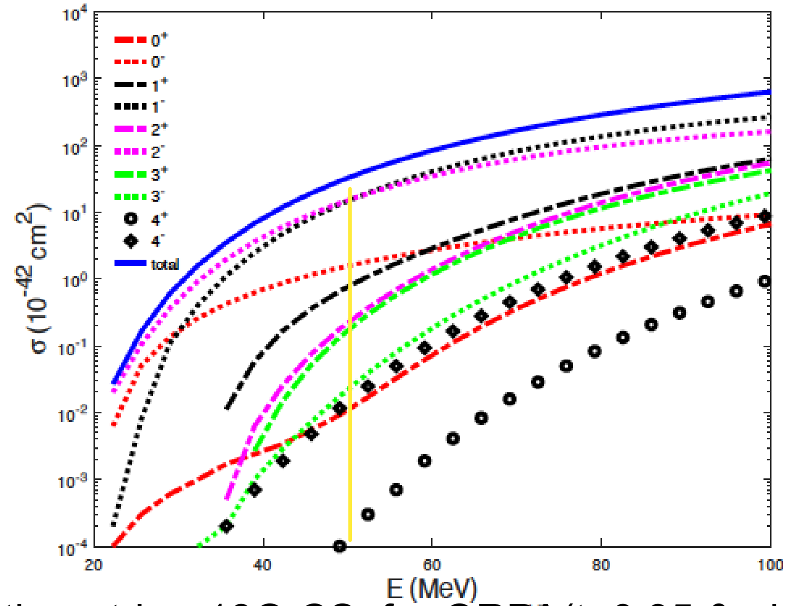

Neutrino-18O CS for QRPA(t=0.35 & ph1)

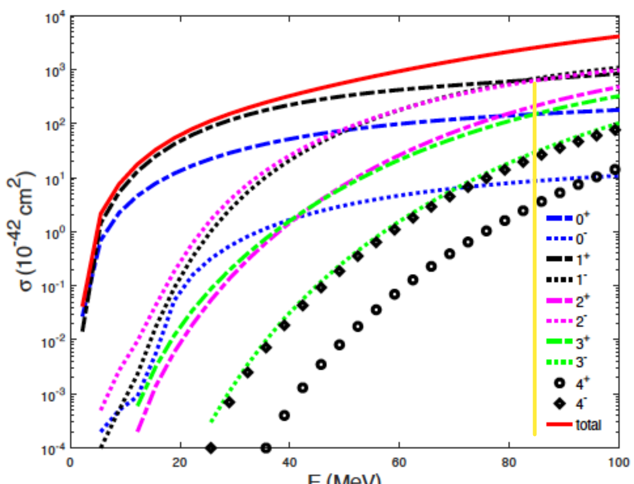

Anti-neutrino-18O CS for QRPA(t=0.35 & ph1)

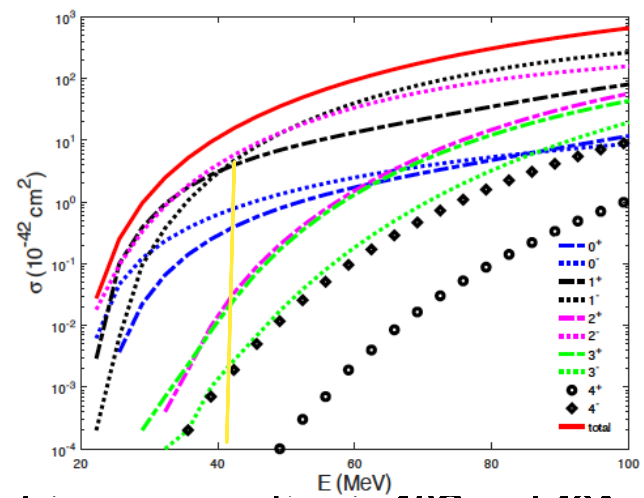

Summary

- Due the universality of the weak hamiltonian, the nuclear models must be describe reasonably good the weak processes: GT strengths for β+ and β- (low energy region up to 40 MeV) and the inclusive muon capture rates (up to 100 MeV).

- A fine tuning could be require an agreement with exclusive reactions, as such as exclusive muon capture rates to first lowest states. Scarce available data for 40Ar or 18O (only inclusive λ) .

- There are several parameters in the nuclear model, one of the most more important is $\mathbf{g_A}$ that goes from 1 to 1.27. Improve the theoretical calculations.

- In LArTPC detectors the most relevant cross is CC 40Ar(v_e,e-)40K that has never been measured experimentally. Recommendations of DUNE work (PRD107,112021 (2023)) can solve this issue.

Acknowlegments

IN ALTUM

fapesb
Fundação de Amparo
à Pesquisa do Estado da Bahia

CAPES

CNPq
Conselho Nacional de Desenvolvimento
Científico e Tecnológico

UNIVERSIDAD NACIONAL DE LA PLATA
PRO SCIENTIA ET PATRIA

TEXAS A&M UNIVERSITY COMMERCE

UNIVERSITAS STUDIORUM ZAGRABIENSIS
MDCLXIX

INSTITUTE for NUCLEAR THEORY

Neutrino/antineutrino cross sections ^{56}Fe

QRPA/PQRPA in ^{56}Fe

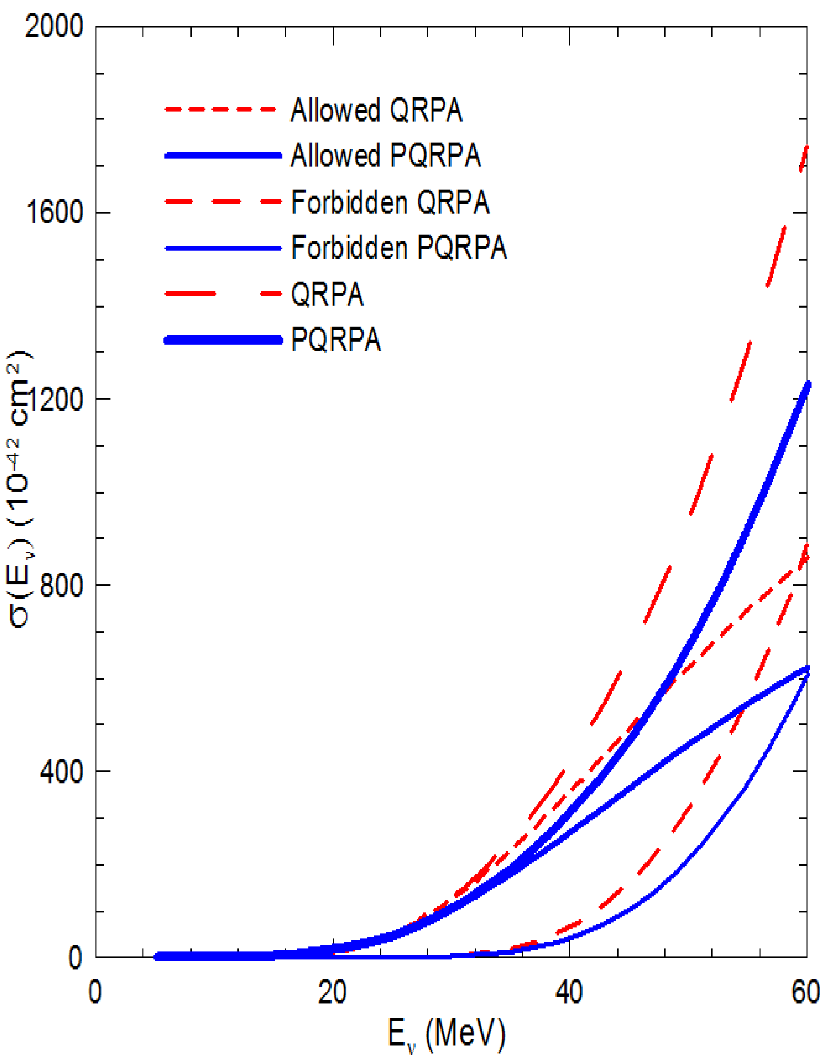

PQRPA & QRPA, PRC 78, 024312 (2008)

RQRPA DD-ME2 , PRC 77,024608 (2008)